US005366695A

United States Patent [19]

Erickson

[11] Patent Number: 5,366,695

[45] Date of Patent: Nov. 22, 1994

[54] **SINGLE CRYSTAL NICKEL-BASED SUPERALLOY**

[75] Inventor: **Gary L. Erickson**, Muskegon, Mich.

[73] Assignee: **Cannon-Muskegon Corporation**, Muskegon, Mich.

[21] Appl. No.: **905,462**

[22] Filed: **Jun. 29, 1992**

[51] **Int. Cl.**[5] **C22C 19/05**

[52] **U.S. Cl.** ..... **420/448**; 420/443; 148/404; 148/410; 415/200; 416/241 R

[58] **Field of Search** ..... 148/404, 410, 428; 420/443, 448; 415/200; 416/241 R, 223 R

[56] **References Cited**

U.S. PATENT DOCUMENTS

Re. 29,920	2/1979	Baldwin	420/448
3,765,879	10/1973	Hockin et al.	420/448
4,045,255	8/1977	Jackson	148/404
4,055,447	10/1977	Jackson	148/404
4,116,723	9/1978	Gell et al.	148/410
4,169,742	10/1979	Wukusick et al.	148/410
4,209,348	6/1980	Duhl et al.	148/410
4,222,794	9/1980	Schweizer et al.	148/410
4,292,076	9/1981	Gigliotti et al.	148/410
4,371,404	2/1983	Duhl et al.	148/409
4,402,772	9/1983	Duhl et al.	148/404
4,492,672	1/1985	Duhl et al.	420/448
4,643,782	2/1987	Harris et al.	148/404
4,677,035	6/1987	Fiedler et al.	148/404
4,719,080	1/1988	Duhl et al.	148/404
4,801,513	1/1989	Duhl et al.	148/404
4,849,030	7/1989	Darolia et al.	148/404
4,888,069	12/1989	Duhl et al.	148/404
4,908,183	3/1990	Chin et al.	148/404
4,915,907	4/1990	Shah et al.	148/404
5,035,958	7/1991	Jackson et al.	420/448
5,043,138	8/1991	Darolia et al.	420/443
5,068,084	11/1991	Cetel et al.	420/443
5,100,484	3/1992	Wukusick et al.	148/410

FOREIGN PATENT DOCUMENTS

2029539	11/1990	Canada .	
240451	10/1987	European Pat. Off.	148/404
2234521	2/1991	United Kingdom .	
2235697	3/1991	United Kingdom .	

OTHER PUBLICATIONS

H. J. Murphy; C. T. Sims and A. M. Beltran, "Phacomp Revisited" International Symposium on Structural Stability in Superalloys Sep. 1968.

Primary Examiner—Melvyn J. Andrews
Assistant Examiner—Margery S. Phipps
Attorney, Agent, or Firm—James D. Dee

[57] **ABSTRACT**

This invention relates to a nickel-based superalloy comprising the following elements in percent by weight: from about 5.0 to about 7.0 percent rhenium, from about 1.8 to about 4.0 percent chromium, from about 1.5 to about 9.0 percent cobalt, from about 7.0 to about 10.0 percent tantalum, from about 3.5 to about 7.5 percent tungsten, from about 5.0 to about 7.0 percent aluminum, from about 0.1 to about 1.2 percent titanium, from about 0 to about 0.5 percent columbium, from about 0.25 to about 2.0 percent molybdenum, from about 0 to about 0.15 percent hafnium, and the balance nickel+incidental impurities, the superalloy having a phasial stability number N_{v3B} less than about 2.10.

32 Claims, 1 Drawing Sheet

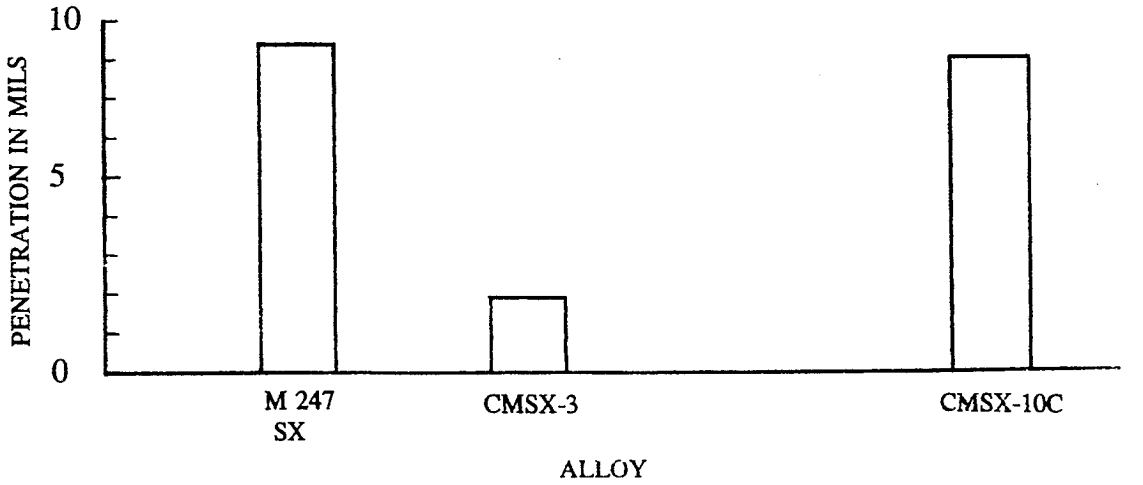

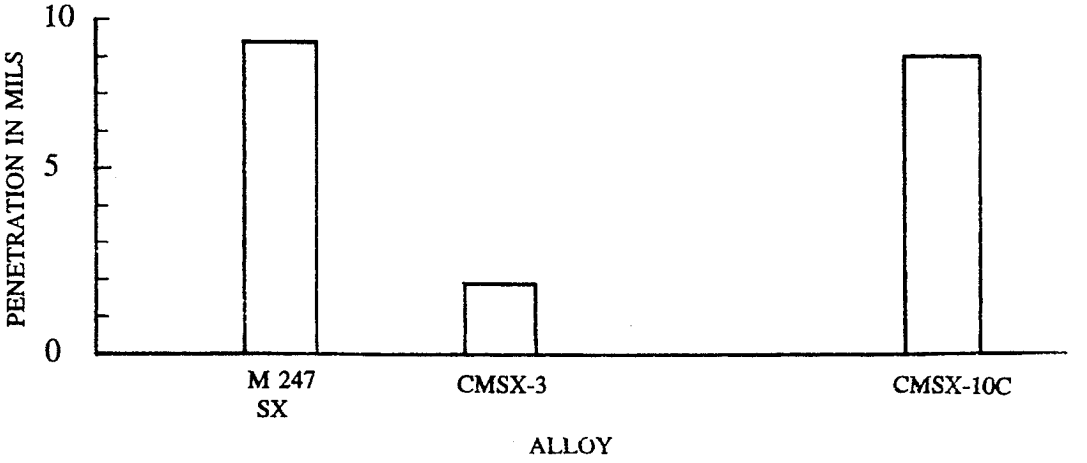
10
5
0
PENETRATION IN MILS
M 247
SX
CMSX-3
CMSX-10C
ALLOY

Fig. 1

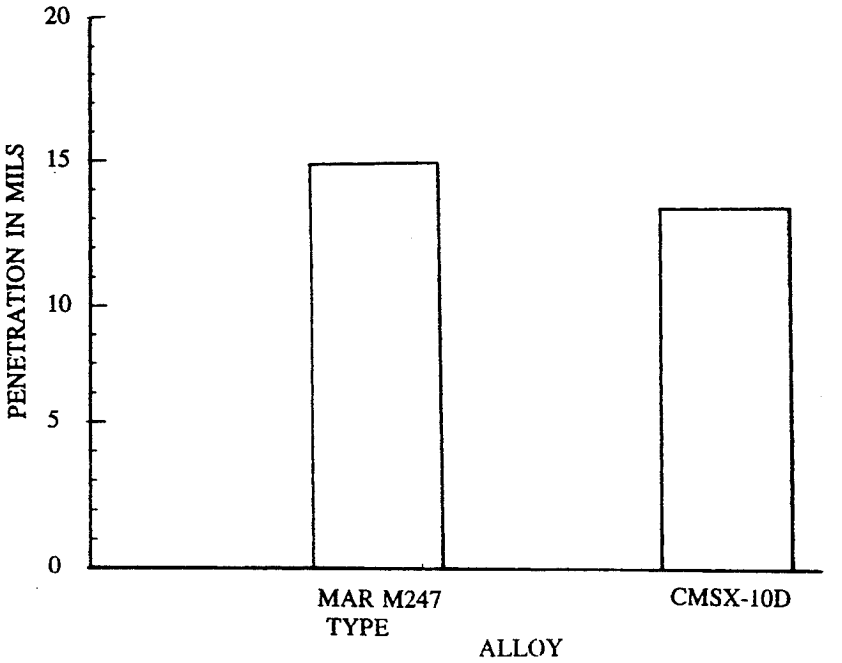
20
15
10
5
0
PENETRATION IN MILS
MAR M247
TYPE
CMSX-10D
ALLOY

Fig. 2

SINGLE CRYSTAL NICKEL-BASED SUPERALLOY

BACKGROUND OF THE INVENTION

1. Field of the Invention

This invention relates to single crystal nickel-based superalloys and, more particularly, single crystal nickel-based superalloys and articles made therefrom for use in advanced gas turbine engines under high stress, high temperature conditions.

2. Description of the Prior Art

Advances over recent years in the metal temperature and stress capability of single crystal articles have been the result of the continuing development of single crystal superalloys, as well as improvements in casting processes and engine application technology. These single crystal superalloy articles include rotating and stationary turbine blades and vanes found in the hot sections of gas turbine engines. However, gas turbine engine design goals have remained the same during the past decades. These goals include the desire to increase engine operating temperature, rotational speed, thrust-to-weight ratio, fuel efficiency, and engine component durability and reliability.

The basic technology of alloys for the casting of single crystal components is described in U.S. Pat. Nos. 3,494,709; 4,116,723 and 4,209,348. Development work resulted in first generation nickel-based superalloys, which were materially improved over those described in the aforementioned patents. However, these first generation nickel-based superalloys contained no rhenium. Examples of such first generation nickel-based superalloys, commercially known as CMSX-2 alloy and CMSX-3 alloy produced by Cannon-Muskegon Corporation, assignee of the present application, are described in U.S. Pat. No. 4,582,548. Further development work resulted in second generation nickel-based superalloys having improved creep strength/creep rate. These second generation nickel-based superalloys have a moderate rhenium content of about 3 weight percent. An example of such a second generation nickel-based superalloy is described in U.S. Pat. No. 4,643,782. This patent discloses a superalloy, commercially known as CMSX-4 alloy, having a specific nickel-based composition including a rhenium content in the range of 2.8–3.2 weight percent. The present invention provides the next generation of nickel-based superalloys having higher total refractory element (W+Re+Mo+Ta) content and improved mechanical properties.

Single crystal articles are generally produced having the low-modulus (001) crystallographic orientation parallel to the component dendritic growth pattern or blade stacking fault axis. Face-centered cubic (FCC) superalloy single crystals grown in the (001) direction provide extremely good thermal fatigue resistance relative to conventionally cast articles. Since these single crystal articles have no grain boundaries, alloy design without grain boundary strengtheners, such as carbon, boron and zirconium, is possible. As these elements are alloy melting point depressants, their reduction from an alloy design provides a greater potential for high temperature mechanical strength achievement since more complete gamma prime solution and microstructural homogenization can be achieved relative to directionally solidified (DS) columnar grain and conventionally cast materials. Their reduction also makes possible a higher incipient melting temperature.

These process benefits are not necessarily realized unless a multi-faceted alloy design approach is undertaken. Alloys must be designed to avoid tendency for casting defect formation such as freckles, slivers, spurious grains and recrystallization. Additionally, the alloys must provide an adequate heat treatment window (numeric difference between an alloy's gamma prime solvus and incipient melting point) to allow for nearly complete gamma prime solutioning. At the same time, the alloy compositional balance should be designed to provide an adequate blend of engineering properties necessary for operation in gas turbine engines. Selected properties generally considered important by gas turbine engine designers include: elevated temperature creep-rupture strength, thermo-mechanical fatigue resistance, impact resistance plus hot corrosion and oxidation resistance.

An alloy designer can attempt to improve one or two of these design properties by adjusting the compositional balance of known superalloys. However, it is extremely difficult to improve more than one or two of the design properties without significantly or even severely compromising the remaining properties. The unique superalloy of the present invention provides an excellent blend of the properties necessary for use in producing single crystal articles for operation in gas turbine engine hot sections.

SUMMARY OF THE INVENTION

This invention relates to a nickel-based superalloy comprising the following elements in percent by weight: from about 5.0 to about 7.0 percent rhenium, from about 1.8 to about 4.0 percent chromium, from about 1.5 to about 9.0 percent cobalt, from about 7.0 to about 10.0 percent tantalum, from about 3.5 to about 7.5 percent tungsten, from about 5.0 to about 7.0 percent aluminum, from about 0.1 to about 1.2 percent titanium, from about 0 to about 0.5 percent columbium, from about 0.25 to about 2.0 percent molybdenum, from about 0 to about 0.15 percent hafnium, and the balance nickel plus incidental impurities, the superalloy having a phasial stability number N_{v3B} less than about 2.10.

Advantageously, this superalloy composition may be further comprised of (percentages are in weight percent) from about 0 to about 0.04 percent carbon, from about 0 to about 0.01 percent boron, from about 0 to about 0.01 percent yttrium, from about 0 to about 0.01 percent cerium and from about 0 to about 0.01 percent lanthanum. Although incidental impurities should be kept to the least amount possible, the superalloy can also be comprised of from about 0 to about 0.04 percent manganese, from about 0 to about 0.05 percent silicon, from about 0 to about 0.01 percent zirconium, from about 0 to about 0.001 percent sulfur, and from about 0 to about 0.10 percent vanadium. In all cases, the base element is nickel. Furthermore, this superalloy can advantageously have a phasial stability number N_{v3B} less than about 1.85, and a chromium content of from about 1.8 to about 3.0 percent, a rhenium content of from about 5.5 to about 6.5 percent, and a cobalt content of from about 2.0 to about 5.0 percent. This invention provides a superalloy having an increased resistance to creep under high stress, high temperature conditions, particularly up to about 1975° F.

Single crystal articles can be suitably made from the superalloy of this invention. The article can be a component for a turbine engine and, more particularly, the

component can be a gas turbine blade or gas turbine vane.

The superalloy compositions of this invention have a critically balanced alloy chemistry which results in a unique blend of desirable properties. These properties include: excellent single crystal component castability, particularly for moderately sized blade and vane components; adequate cast component solutionability; excellent resistance to single crystal cast component recrystallization; ultra-high creep-rupture strength to about 1975° F.; extremely good low cycle fatigue strength; extremely good high cycle fatigue strength; high impact strength; very good bare hot corrosion resistance; very good bare oxidation resistance; and adequate microstructural stability, such as resistance to the undesirable, brittle phases called topologically close-packed (TCP) phases.

Accordingly, it is an object of the present to provide superalloy compositions and single crystal articles made therefrom having a unique blend of desirable properties. It is a further object of the present invention to provide superalloys and single crystal articles made therefrom for use in advanced gas turbine engines under high stress, high temperature conditions, such as up to about 1975° F. These and other objects and advantages of the present invention will be apparent to those skilled in the art upon reference to the following description of the preferred embodiments.

BRIEF DESCRIPTION OF THE DRAWINGS

FIG. 1 is a chart of hot corrosion test results performed to 117 hours on one embodiment of the alloy of this invention and on two prior art alloys;

FIG. 2 is a chart of hot corrosion test results performed to 144 hours on another embodiment of the alloy of this invention and on a prior art alloy.

DESCRIPTION OF THE PREFERRED EMBODIMENTS

The nickel-based superalloy of the present invention comprises the following elements in percent by weight:

Rhenium	about 5.0–7.0
Chromium	about 1.8–4.0
Cobalt	about 1.5–9.0
Tantalum	about 7.0–10.0
Tungsten	about 3.5–7.5
Aluminum	about 5.0–7.0
Titanium	about 0.1–1.2
Columbium	about 0–0.5
Molybdenum	about 0.25–2.0
Hafnium	about 0–0.15
Nickel + Incidental Impurities	balance

This superalloy composition also has a phasial stability number N_{v3B} less than about 2.10. Further, this invention has a critically balanced alloy chemistry which results in a unique blend of desirable properties. These properties include increased creep-rupture strength relative to prior art single crystal superalloys, single crystal component castability, cast component solutionability, single crystal component resistance to recrystallization, fatigue strength, impact strength, bare hot corrosion resistance, bare oxidation resistance, and microstructural stability, including resistance to TCP phase formation under high stress, high temperature conditions,

Unlike prior nickel-based superalloys known in the art, the superalloys of the present invention have a low chromium, low cobalt and high rhenium content. The chromium is about 1.8–4.0% by weight. Advantageously, the chromium content is from 1.8% to 3.0% by weight. This chromium content is significantly lower than that typically found in prior art single crystal nickel-based superalloys. In the present superalloy, chromium provides hot corrosion resistance, although it may also assist with the alloy's oxidation capability. Tantalum and rhenium also assist toward hot corrosion property attainment, and aluminum is present at sufficient levels to provide adequate oxidation resistance, so that relatively low addition of chromium is tolerable in this alloy. Besides lowering the alloy's gamma prime solvus, chromium contributes to the formation of Cr, Re, W-rich TCP phase and must be balanced accordingly in these compositions.

The cobalt content is about 1.5–9.0% by weight. Advantageously, the cobalt content is from 2.0% to 5.0% by weight. This cobalt content is lower than that typically found in prior art single crystal nickel-based superalloys. In the present superalloy, cobalt assists in providing an appropriate heat treatment window since it has the effect of lowering the alloy's gamma prime solvus while generally not affecting its incipient melting point. Rhenium-containing alloys are generally designed with much higher cobalt content than the present invention for the purpose of imparting increased solid solubility and phasial stability. However, the superalloys of the present invention unexpectedly show that much lower cobalt contents are possible and desirable toward providing optimized phasial stability, including control of TCP phase formation.

The rhenium content is about 5.0–7.0% by weight and, advantageously, rhenium is present in an amount of from 5.5% to 6.5% by weight. The amount of rhenium in the superalloy of the present invention is significantly greater than the rhenium content of prior art single crystal nickel-based superalloys. Furthermore, the superalloys of this invention are generally designed with an increased level of refractory element content, e.g., W+Re+Mo+Ta. The tungsten content is about 3.5–7.5% by weight and, advantageously, the amount of tungsten is from 3.5% to 6.5% by weight. Tungsten is added since it is an effective solid solution strengthener and it contributes to strengthening the gamma prime. Additionally, tungsten is effective in raising the alloy's incipient melting temperature. The amount of tungsten added to these superalloys is balanced with the amount of rhenium added since they both contribute to, the formation of "freckle" defects during the single crystal investment casting process. They also both strongly effect the propensity for TCP phase formation.

Similar to tungsten, rhenium is effective in raising the alloy's incipient melting point. However, rhenium is a more effective strengthener than tungsten, molybdenum and tantalum in terms of elevated temperature creep-rupture and, therefore, rhenium is added appropriately. Additionally, rhenium has a positive influence on this alloy's hot corrosion resistance. Moreover, rhenium partitions primarily to the gamma matrix, and it is effective in slowing gamma prime particle growth during high temperature, high stress conditions. Besides requiring the balancing of rhenium with tungsten for castability reasons, W+Re must also be set at a level consistent with minimizing TCP phase formation. In general, the TCP phases which occur in such material

are rich in chromium, tungsten, and rhenium content, with rhenium being present in the greatest proportion. Thus, careful Re/W ratio control is necessary in this alloy to control the propensity for TCP phase formation.

The molybdenum content is about 0.25–2.0% by weight. Advantageously, molybdenum is present in an amount of from 0.25% to 1.5% by weight. Molybdenum is a good solid solution strengthener, but it is not as effective as tungsten, rhenium and tantalum. However, since the alloy's density is always a design consideration, and the molybdenum atom is lighter than the other solid solution strengtheners, the addition of molybdenum is a means of assisting control of the overall alloy density in the compositions of this invention.

The tantalum content is about 7.0–10.0% by weight and, advantageously, the tantalum content is from 8.0% to 10.0% by weight. Tantalum is a significant contributor to this alloy's strength through means of solid solution strengthening and enhancement of gamma prime particle strength (tantalum also partitions to the gamma prime phase). In this alloy, tantalum is able to be utilized at relatively high concentration since it does not contribute to TCP phase formation. Additionally, tantalum is an attractive single crystal alloy additive in this composition since it assists in preventing "freckle" defect formation during the single crystal casting process. Tantalum is also beneficial in this composition since it tends to raise this alloy's gamma prime solvus, and it is effective toward promoting good alloy oxidation and hot corrosion resistance, along with aluminide coating durability.

The aluminum content is about 5.0–7.0% by weight. Furthermore, the amount of aluminum present in this composition is advantageously from 5.3% to 6.5% by weight. Aluminum and titanium are the primary elements comprising the gamma prime phase. These elements are added in this composition in a proportion and ratio consistent with achieving adequate alloy castability, solution heat treatability, phasial stability and high mechanical strength. Aluminum is also added to this alloy in proportions sufficient to provide oxidation resistance.

The titanium content is about 0.1–1.2% by weight. Advantageously, titanium is present in this composition in an amount from 0.2% to 0.8% by weight. Titanium is generally beneficial to the alloy's hot corrosion resistance, but it can have a negative effect to oxidation resistance, alloy castability and alloy response to solution heat treatment. Accordingly, the titanium content must be maintained within the stated range of this composition.

The columbium content is about 0–0.5% by weight and, advantageously, the columbium content is from 0 to 0.3% by weight. Columbium is a gamma prime forming element and it is an effective strengthener in the nickel-based superalloys of this invention. Generally, however, columbium is a detriment to alloy oxidation and hot corrosion properties, so its addition to the composition of this invention is minimized. Moreover, columbium is added to this invention's composition for the purpose of gettering carbon, which can be chemisorbed into component surfaces during non-optimized vacuum solution heat treatment procedures. Any carbon pick-up will tend to form columbium carbide instead of titanium or tantalum carbide, thereby preserving the greatest proportion of titanium and/or tantalum for gamma prime and/or solid solution strengthening in this alloy.

The hafnium content is about 0–0.15% by weight and, advantageously, hafnium is present in an amount from 0.02 to 0.05% by weight. Hafnium is added in a small proportion to the present composition in order to assist with coating adherence. Hafnium generally partitions to the gamma prime phase.

The balance of this invention's superalloy composition is comprised of nickel and small amounts of incidental impurities. Generally, these incidental impurities are entrained from the industrial process of production, and they should be kept to the least amount possible in the composition so that they do not affect the advantageous aspects of the superalloy. For example, these incidental impurities may include up to about 0.04% by weight manganese, up to about 0.05% by weight silicon, up to about 0.01% by weight zirconium, up to about 0.001% by weight sulfur, and up to about 0.10% by weight vanadium. Amounts of these impurities which exceed the stated amounts could have an adverse effect upon the resulting alloy's properties.

Additionally, the superalloy may optionally contain about 0–0.04% by weight carbon, about 0–0.01% by weight boron, about 0–0.01% by weight yttrium, about 0–0.01% by weight cerium and about 0–0.01% by weight lanthanum.

Not only does the superalloy of this invention have a composition within the above specified ranges, but it also has a phasial stability number N_{v3B} less than about 2.10. Advantageously, the phasial stability number N_{v3B} is less than 1.85 and, preferably, the phasial stability number N_{v3B} is less than 1.75. As can be appreciated by those skilled in the art, N_{v3B} is defined by the PWA N-35 method of nickel-based alloy electron vacancy TCP phase control factor calculation. This calculation is as follows:

EQUATION 1

Conversion for weight percent to atomic percent:

$$\text{Atomic percent of element } i = Pi = \frac{Wi/Ai}{\Sigma i(Wi/Ai)} \times 100$$

where: Wi=weight percent of element i
Ai=atomic weight of element i

EQUATION 2

Calculation for the amount of each element present in the continuous matrix phase:

Element	Atomic amount Rii remaining
Cr	$R_{Cr} = 0.97P_{Cr} - 0.375P_B - 1.75P_C$
Ni	$R_{Ni} = P_{Ni} + 0.525P_B - 3(P_{Al} + 0.03P_{Cr} + P_{Ti} - 0.5P_C + 0.5P_V + P_{Ta} + P_{Cb} + P_{Hf})$
Ti, Al, B, C, Ta, Cb, Hf	$Ri = O$
V	$Rv = 0.5P_V$
W	$*R_{(W)} = P_W - 0.167P_C \frac{P_W}{P_{Mo} + P_W}$
Mo	$R_{(Mo)} = P_{(Mo)} - 0.75P_B - 0.167P_C \frac{P_{Mo}}{(P_{Mo} + P_W)}$

*Note:
weight percentage Re is added to weight percentage W for the calculation above.

EQUATION 3

Calculation of N_{v3B} using atomic factors from Equations 1 and 2 above:

$$N_i^i = \frac{R_i}{{}_iR_i} \quad \text{then} \quad N_{v3B} = \Sigma_i Ni(N_v)i$$

where: i=each individual element in turn.
$N_i i$=the atomic factor of each element in matrix.
(N_v) i=the electron vacancy No. of each respective element.

This calculation is exemplified in detail in a technical paper entitled "PHACOMP Revisited", by H. J. Murphy, C. T. Sims and A. M. Beltran, published in Volume 1 of International Symposium on Structural Stability in Superalloys (1968), the disclosure which is incorporated by reference herein. As can be appreciated by those skilled in the art, the phasial stability number for the superalloys of this invention is critical and must be less than the stated maximum to provide a stable microstructure and capability for the desired properties under high temperature, high stress conditions. The phasial stability number can be determined empirically, once the practitioner skilled in the art is in possession of the present subject matter.

The superalloy of this invention can be used to suitably make single crystal articles, such as components for turbine engines. Preferably, this superalloy is utilized to make a single crystal casting to be used under high stress, high temperature conditions characterized by an increased resistance to creep under such conditions, particularly high temperature conditions up to about 1975° F. While this superalloy can be used for any purpose requiring high strength castings incorporating a single crystal, its particular use is in the casting of single crystal blades and vanes for gas turbine engines. This alloy possesses an unusual resistance to component recrystallization during solution heat treatment, which is considered an important alloy characteristic that is necessary when producing advanced technology, multipiece, cast bonded single crystal airfoils. Additionally, this superalloy provides the alloy castability characteristics believed necessary to produce conventional-process-cast, moderately-sized turbine airfoils with intricate cooling passages.

While this superalloy's primary use is in aircraft turbine engines, there are stationary engine applications requiring the specialized high performance characteristics of this alloy. This is particularly the case in turbine engines which require performing characteristics with very restricted clearances, thereby materially limiting the amount of permissible creep. Engines designed to develop high performance characteristics are normally operated at higher component temperatures and, therefore, the problem of creep is increased. Generally, creep in excess of 1% is considered unacceptable in these cases. The creep characteristics of known state of the art alloys have limited operating temperatures and, thus, maximum performance capability. The superalloy of this invention has an increased resistance to creep under high stress, high temperature conditions, particularly up to 1975° F.

The single crystal components made from this invention's compositions can be produced by any of the single crystal casting techniques known in the art. For example, single crystal directional solidification processes can be utilized, such as the seed crystal process and the choke process.

The single crystal castings made from the superalloy of the present invention are advantageously subjected to a high temperature aging heat treatment in order to optimize the creep-rupture properties of these alloys. This invention's single crystal castings can be aged at a temperature of from about 1950° F. to about 2125° F. for about 1 to about 20 hours. However, as can be appreciated by those skilled in the art, the optimum aging temperature and time for aging depends on the precise composition of the superalloy.

This invention provides superalloy compositions having a unique blend of desirable properties. These properties include: excellent single crystal component castability, particularly for moderately sized blade and vane components; excellent cast component solutionability; excellent resistance to single crystal cast component recrystallization ultra-high creep-rupture strength to about 1975° F.; extremely good low cycle fatigue strength; extremely good high cycle fatigue strength; high impact strength; very good bare hot corrosion resistance; very good bare oxidation resistance; and microstructural stability, such as resistance to formation of the undesirable TCP phases. As noted above, this superalloy has a precise composition with only small permissible variations in any one element if the unique blend of properties is to be maintained.

In order to more clearly illustrate this invention and provide a comparison with representative superalloys outside the claimed scope of the invention, the examples set forth below are presented. The following examples are included as being illustrations of the invention and its relation to other superalloys and articles, and should not be construed as limiting the scope thereof.

EXAMPLES

A large number of superalloy test materials were prepared to investigate the compositional variations and ranges for the superalloys of the present invention. Some of the alloy compositions tested and reported below fall outside the claimed scope of the present invention, but are included for comparative purposes to assist in the understanding of the invention. Representative alloy aim chemistries of those materials tested are reported in Table I below.

TABLE 1

Alloy	C	B	Cr	Co	Mo	W	Cb	Ti	Al	Ta	Re	Hf	Ni	Nv3B*	See "Key" Below 1	2	3	4
CMSX -10A	—	—	3.0	8.5	.70	7.2	.30	.65	6.0	7.6	5.0	.05	BAL	2.08	12.46	6.65	14.55	20.76
-10B	—	—	2.6	8.2	.70	6.95	.30	.68	6.0	7.9	4.95	.06	BAL	2.02	11.9	6.68	14.88	20.5
-10C	—	—	2.5	7.7	.70	6.6	.30	.65	5.9	8.2	4.8	.05	BAL	1.90	11.4	6.55	15.05	20.3
-10D	—	—	4.0	4.8	.60	6.4	.30	.60	5.7	8.2	4.9	.03	BAL	1.95	11.3	6.30	14.80	20.1
-10E	—	—	2.2	7.2	.70	6.3	.25	.72	5.85	8.3	4.8	.042	BAL	1.84	11.1	6.57	15.12	20.1
-10F	.02	.02	2.4	7.6	.65	6.45	.28	.63	5.9	8.5	5.0	.046	BAL	1.89	11.45	6.53	15.31	20.6
-10G	—	—	2.4	6.3	.50	6.4	.20	.70	5.8	8.0	5.5	.04	BAL	1.82	11.9	6.5	14.7	20.4
-10Ga	—	—	2.4	4.0	.50	6.2	.15	.55	5.8	8.3	5.6	.04	BAL	1.72	11.8	6.35	14.8	20.6
10K -10Gb	—	—	2.3	3.3	.40	5.5	.10	.30	5.7	8.4	6.3	.03	BAL	1.60	11.8	6.0	14.5	20.6

TABLE 1-continued

Alloy	C	B	Cr	Co	Mo	W	Cb	Ti	Al	Ta	Re	Hf	Ni	Nv3B*	See "Key" Below 1	2	3	4
-10H	—	—	2.2	5.9	.50	6.4	.15	.80	5.9	8.0	5.5	.04	BAL	1.82	11.9	6.7	14.85	20.4
-10I	—	—	2.5	4.7	.50	6.4	.15	.70	5.8	7.9	6.0	.04	BAL	1.81	12.4	6.5	14.65	20.9
-10Ia	—	—	2.5	3.3	.40	6.1	.10	.60	5.8	7.9	6.0	.04	BAL	1.69	12.1	6.4	14.4	20.4
-10J	.015	.01	2.65	4.0	.50	6.0	.20	.65	5.8	9.0	5.5	.04	BAL	1.79	11.5	6.45	15.65	21.0
-10L	—	—	2.0	2.7	.40	5.3	.10	.20	5.65	8.4	6.3	.03	BAL	1.50	11.6	5.85	14.35	20.4
CMSX -12A	—	—	3.0	4.5	.35	5.5	—	1.0	5.65	9.0	5.5	.04	BAL	1.84	11.0	6.65	15.65	20.35
-12B	—	—	3.5	3.0	.35	5.0	—	.90	5.60	8.8	6.0	.04	BAL	1.80	11.0	6.5	15.3	20.15
-12C	—	—	2.8	3.5	.40	5.3	—	.75	5.60	8.8	5.8	.04	BAL	1.70	11.1	6.35	15.15	20.3
12D -12Ca	—	—	2.5	3.2	.45	4.7	—	.50	5.60	8.7	6.3	.03	BAL	1.61	11.0	6.10	14.8	20.15
-12E	—	—	2.0	3.0	.45	4.7	—	.40	5.60	8.7	6.3	.03	BAL	1.50	11.0	6.0	14.7	20.15
CMSX -10Ri	—	—	2.65	7.0	.60	6.4	.40	.80	5.8	7.5	5.5	.06	BAL	1.91	11.9	6.6	14.5	20.0
CMSX -12Ri	—	—	3.4	8.0	.50	6.0	—	1.0	5.6	7.6	5.3	.06	BAL	1.92	11.3	6.6	14.6	19.4

Key:
1-W + Re
2-Al + Ti
3-Al + Ti + Ta + Cb
4-W + Re + Mo + Ta
*Calculated using PWA N-35 Method

Third generation single crystal alloy development to investigate the compositional variations for the superalloys of the present invention began with the definition and evaluation of a series of experimental compositions. Increased creep-rupture strength was the primary objective of the initial development effort, with elemental balancing to provide a combination of useful engineering characteristics following the definition of a base concept for increased strength.

The initial materials explored the utility of higher levels of refractory element and gamma prime forming elements than are present in similar prior art compositions. As shown in Table 1, the alloy chromium content was reduced to improve alloy stability. Cobalt content, initially thought to be required for increased solid solubility, could be significantly reduced. Refractory element content (W+Re+Mo+Ta) was varied, while the summation of the primary gamma prime partitioning elements (Ai+Ti+Ta+Cb) was also varied. The alloy's Re content was initially explored at conventional levels, but it was found that the Re level had to be increased.

Standard N_{v3B} calculations were performed during the initial alloy design stage to assist respective alloy phasial stability predictions, with that number varying from one alloy composition to another.

Some of the alloys were produced using production-type procedures. These alloys were vacuum induction melted in the Cannon-Muskegon Corporation V-1 furnace, yielding approximately 200–300 lbs, of bar product per alloy (see Table 2 below). Quantities of each compositional iteration, as reported in Table 2, were made into test bars and test blades by vacuum investment casting. Solution heat treatment procedures were developed in the laboratory in 3" and 6" diameter tube furnaces. Gamma prime aging treatments were also performed in the laboratory.

TABLE 2

Alloy	Heat No.	V-1 VIM FURNACE HEAT CHEMISTRIES C	B	Cr	Co	Mo	W	Cb	Ti	Al	Ta	Re	Nf	Ni
CMSX -10A	VF 778	.001	<.001	2.9	8.5	.7	7.2	.3	.70	6.05	7.6	5.0	.05	BASE
-10B	VF 831	.002	<.001	2.6	8.2	.7	6.9	.3	.68	6.06	7.9	4.9	.05	BASE
-10Ri	VF 965	.001	<.001	2.65	7.0	.6	6.4	.4	.80	5.72	7.6	5.5	.06	BASE
-10Ri	VF 966	.001	<.001	2.69	7.0	.6	6.3	.4	.80	5.66	7.6	5.4	.06	BASE
-10Ri	VF 980	.001	<.001	2.66	7.0	.6	6.3	.4	.79	5.78	7.6	5.4	.06	BASE
-12Ri	VF 963	.001	<.001	3.3	8.0	.48	6.0	<.05	1.01	5.69	7.6	5.3	.07	BASE
-12Ri	VF 964	.001	<.001	3.4	8.0	.48	6.1	<.05	1.00	5.60	7.6	5.3	.06	BASE
-12Ri	VF 979	.001	<.001	3.4	8.0	.50	6.1	<.05	1.00	5.56	7.6	5.3	.06	BASE
-10Ga	VF 983	.001	<.001	2.4	3.95	.41	6.1	.14	.56	5.83	8.4	5.9	.03	BASE
-12C	VF 985	.001	<.001	2.7	3.5	.45	5.3	<.05	.75	5.66	8.8	6.0	.025	BASE
-10Gb (-10K)	VF 994	.001	<.001	2.2	3.3	.40	5.5	.09	.24	5.74	8.2	6.4	.025	BASE
-12Ca (-12D)	VF 993	.001	<.001	2.4	3.2	.46	4.8	<.01	.50	5.64	8.6	6.4	.025	BASE

All other specimens reported in Table 1 above were produced by blending base alloy bar stock with the virgin elemental additions necessary to achieve the desired composition. The blending was done during test bar and blade manufacture. The base alloy bar stock plus virgin additions were placed into the casting furnace melt crucible, melted and the bath homogenized prior to pouring into an appropriate shell mold. It is believed that good correlation between alloy aim chemistry and test bar/blade chemistry was routinely achieved (see Table 3 below).

TABLE 3

Alloy	C	B	Cr	Co	Mo	W	Cb	Ti	Al	Ta	Re	Hf	Ni	Nv3B*
CMSX -10A	—	—	2.9	8.5	.68	7.4	.29	.69	6.0	7.5	5.1	.07	BAL	2.09
-10B	—	—	2.7	8.1	.69	6.95	.29	.69	6.0	7.8	4.8	.06	BAL	2.01
-10C	—	—	2.6	7.7	.69	6.4	.30	.62	5.7	8.3	4.7	.07	BAL	1.86
-10D	—	—	4.0	5.0	.62	6.0	.31	.59	5.44	8.1	4.7	.04	BAL	1.83
-10E	—	—	2.2	7.2	.70	6.4	.26	.63	5.89	8.2	4.8	.05	BAL	1.84
-10F	.014	.027	2.4	7.7	.65	6.4	.28	.63	5.96	7.9	5.0	.04	BAL	1.86
-10G	—	—	2.5	6.5	.53	5.5	.20	.68	5.6	8.2	4.6	.05	BAL	1.68
-10Ga	—	—	2.4	4.0	.41	6.2	.14	.55	5.79	8.3	6.0	.025	BAL	1.73

TABLE 3-continued

Alloy	C	B	Cr	Co	Mo	W	Cb	Ti	Al	Ta	Re	Hf	Ni	Nv3B*
-10Gb (10K)	—	—	2.3	3.5	.42	5.9	.10	.43	5.67	8.5	6.0	.024	BAL	1.63
-10H	—	—	2.3	5.6	.51	6.2	.17	.76	5.58	7.8	5.4	.05	BAL	1.69
-10I	—	—	2.6	4.8	.52	6.6	.14	.67	5.65	7.4	5.4	.04	BAL	1.70
-10Ia	—	—	2.7	3.5	.47	5.2	.10	.60	5.80	8.0	5.8	.04	BAL	1.67
-10J	.017	.01	2.6	4.0	.48	6.0	.19	.62	5.74	8.8	5.7	.04	BAL	1.76
-10L	—	—												
-12A	—	—	3.0	4.6	.39	5.3	<.01	.96	5.61	9.4	5.0	.05	BAL	1.80
-12B	—	—	3.5	3.0	.38	5.1	<.01	.84	5.52	8.8	6.1	.05	BAL	1.79
-12C	—	—	2.7	3.5	.45	5.4	<.01	.75	5.62	8.8	6.0	.04	BAL	1.72
-12Ca (12D)	—	—	2.5	3.2	.46	5.0	<.01	.61	5.56	8.7	6.0	.03	BAL	1.60
-12E	—	—												
-10Ri	—	—	2.65	7.0	.60	6.4	.40	.80	5.67	7.6	5.5	.065	BAL	1.87
12Ri	—	—	3.4	8.0	.48	6.1	<.01	.99	5.54	7.6	5.3	.07	BAL	1.92

*PWA N-35 Method

For the CMSX-10D specimen (see Table 1), high quality virgin elemental additions were vacuum melted and the refined material was poured into 2" diameter bars. In turn, a quantity of the resulting bar was used to produce single crystal test bar/blade specimens by investment casting.

It was apparent that considerable variation in the investment casting process integrity may have occurred during specimen manufacture since varying levels of test bar freckle formation, secondary dendrite arm spacing and property attainment were apparent. Derivative alloy response to solution treatment (reported in Table 4 below) varied, and was a function of both alloy composition and test specimen quality.

Heat treatments developed for the alloy iterations are reported in Table 4 below. Full gamma prime solutioning was desired for each material, however, this objective was not universally achieved. Primary gamma prime aging was performed to effect a more desirable gamma prime particle size and distribution. Secondary gamma prime aging was performed to effect precipitation of conventional matrix gamma prime precipitates along with ultra-fine gamma prime precipitates located within the matrix channels between the primary gamma prime particles for these specimens.

TABLE 4

	Heat Treatment Detail				
	Peak Solution Temperature		% γ,	Primary γ,	Secondary γ,
Alloy	°F.	°C.	Solutioned*	Aging+	Aging+
CMSX -10A	2460	1349	97.0–98.0	1975° F./4 Hrs	1600° F./20 + 1400° F./24
-10B	2465	1352	97.0–98.0	1975° F./4 Hrs	1600° F./20 + 1400° F./24
				1975° F./19.5 Hrs	
-10C	2470	1354	99.0–99.5	2100° F./8 Hrs	1600° F./20 + 1400° F./24
				1975° F./10 Hrs	
-10D	2450	1343	99.9–100	1975° F./10 Hrs	1600° F./22 + 1400° F./24
-10E	2465	1352	100	1975° F./15 Hrs	1600° F./20 + 1400° F./24
				1975° F./21 Hrs	1600° F./25.5 + 1400° F./23
-10F	2444	1340	95	1975° F./16 Hrs	1600° F./23 + 1400° F./24
-10G	2475	1357	99.0–99.5	1975° F./12 Hrs	1600° F./24.5 + 1400° F./17
-10Ga	2485–90	1363–65	99.5–100	2075° F./5 Hrs	1600° F./20 + 1400° F./23
				2075° F./6 Hrs	1600° F./24 + 1400° F./30
					1612° F./48 + 1414° F./22
-10Gb(10K)	2485	1363	100	2075° F./6 Hrs	1600° F./24 + 1400° F./30
-10H	2475	1357	98.5–99.0	1975° F./16 Hrs	1600° F./27.5 + 1400° F./27
				1975° F./18 Hrs	1600° F./101 + 1400° F./46
-10I	2475	1357	100	2075° F./5 Hrs	1600° F./22 + 1405° F./24
-10Ia	2480	1360	99.5–100	2075° F./5 Hrs	1600° F./24 + 1400° F./24
-10J	2480	1360	98.0–99.0	1975° F./15 Hrs	1600° F./24 + 1400° F./30
				2075° F./5 Hrs	1600° F./24 + 1400° F./30
-10L					
-12A	2475	1357	98.5–99.0	1975° F./16.5 Hrs	1600° F./24 + 1400° F./32
				1975° F./12 Hrs	1600° F./24 + 1400° F./27.5
-12B	2480	1360	99.0–99.5	1975° F./13 Hrs	1600° F./57 + 1400° F./39
-12C	2485–90	1363–65	99.5–100	2075° F./5 Hrs	1600° F./20 + 1400° F./5
				2075° F./6 Hrs	1600° F./24 + 1400° F./30
-12Ca(12D)	2485	1363	100	2075° F./6 Hrs	1600° F./24 + 1400° F./30
-12E					
-10Ri	2460	1349	98.5–99.8	2075° F./6 Hrs	1600° F./24 + 1400° F./30
-12Ri	2455	1346	100	2075° F./6 Hrs	1600° F./24 + 1400° F./30

*Determined by visual estimation
+Specimens air cooled from all aging treatments

Fully heat treated test bars were creep-rupture tested. The specimens were machined and low-stress ground to ASTM standard proportional specimen dimension. The specimens were creep-rupture tested at various condition of temperature and stress, according to standard ASTM procedure.

A significant factor of the CMSX-10A alloy design was the shift to higher Re content. At the same time, W, Cr, Ta and other gamma prime strengtheners were balanced to provide the desired alloy characteristics and properties. The alloys higher Re level resulted in significantly improved creep-rupture strength throughout the entire test regime, as indicated by the results

reported in Table 5 below for the CMSX-10A specimens.

TABLE 5

CMSX-10A CREEP-RUPTURE

TEST CONDITION	RUPTURE TIME HOURS	% ELONG.	% RA	FINAL CREEP READING t, hours	FINAL CREEP READING % deformation	TIME IN HOURS TO REACH 1.0%	TIME IN HOURS TO REACH 2.0%
1600° F./75.0 ksi	534.4	24.2	26.9	534.2	22.331	10.9	21.0
	328.4	22.0	27.8	328.3	21.055	6.3	8.7
	527.3	21.1	26.3	526.3	17.552	28.4	72.2
1700° F./50.0 ksi	305.0	31.1	34.5	304.2	28.614	62.1	108.9
	292.4	19.2	19.9	291.8	19.324	71.5	123.7
	87.6	2.6	5.8	85.7	1.474	65.9	—
1800° F./30.0 ksi	415.6	16.1	21.4	413.8	15.643	182.7	246.1
	848.0	37.1	33.0	846.3	34.326	460.4	524.3
	1016.2	33.2	30.5	1014.3	32.984	476.8	655.1
1800° F./36.0 ksi	586.5	38.1	38.0	585.6	33.050	395.0	425.0
	572.7	36.9	35.3	570.7	29.029	395.0	422.0
	546.5	26.4	34.2	545.7	25.843	373.0	406.0
	420.3	22.4	26.3	418.7	18.105	286.7	317.6
	426.0	14.8	17.0	425.1	10.244	326.5	353.2
	239.8	24.3	23.8	239.7	23.264	94.1	123.9
	255.7	19.9	27.4	253.6	18.510	115.2	152.7
1900° F./25.0 ksi	32.3	5.5	11.0	31.0	2.075	26.7	30.7
	129.7	43.2	38.9	128.7	39.556	30.4	48.1
	168.7	34.7	36.4	166.1	30.816	58.2	78.4
	228.1	18.1	32.3	226.4	16.926	146.3	160.6
	277.7	29.5	31.1	276.4	27.323	9.9	29.9
	423.4	39.7	38.3	422.7	35.121	218.4	250.9
	383.8	35.9	36.1	382.7	34.861	192.9	226.7
	373.3	31.3	35.7	371.6	26.138	211.6	238.0
2000° F./18.0 ksi	138.0	22.3	33.0	136.3	19.052	33.9	77.0
	134.9	40.7	36.5	134.7	38.328	54.7	71.9
	122.9	23.2	34.9	122.0	19.050	50.1	69.4
	115.6	34.2	36.6	114.4	30.861	40.8	56.8
	245.2	35.1	36.2	244.3	29.844	135.7	157.9
	221.9	36.3	35.4	221.8	33.737	113.0	140.0
	181.2	32.1	34.2	180.1	29.249	53.1	61.4
2050° F./15.0 ksi	126.4	47.9	49.0	124.1	30.086	45.8	69.8
	150.5	45.5	47.8	148.1	39.308	16.8	34.5
	140.5	30.6	40.0	138.7	23.596	30.6	76.4
	120.8	29.5	39.7	120.0	29.479	16.3	55.6
	79.0	11.7	14.4	79.0	11.644	41.7	54.8
	112.2	24.3	31.3	112.1	21.401	55.9	69.5
2100° F./12.5 ksi	94.1	22.1	27.5	94.1	20.520	42.2	62.6
	112.5	39.4	33.1	112.2	29.126	28.0	58.8
	96.6	25.9	35.9	95.5	14.542	52.3	62.5
	123.6	43.4	40.4	122.9	31.050	40.9	63.5
	50.8	21.7	29.6	49.9	9.330	35.1	37.6
	90.5	41.6	43.7	89.7	37.422	13.6	38.5
1800° F./36.0 ksi*	420.6	23.9	35.1	419.9	23.196	213.8	286.0
	396.1	37.1	34.0	394.7	31.623	239.4	264.9
	384.9	31.1	34.0	382.9	25.554	220.5	247.9

*As-Solutioned Condition

Microstructural review of the failed rupture specimens of this alloy revealed that TCP phase precipitation occurred during the respective creep-rupture tests, particularly those at 1900° F. and above. It became apparent that the N_{v3B} phasial stability number calculation would be an effective tool in predicting alloy stability and, effectively, high temperature creep strength for the invention.

Wherein the CMSX-10A specimen's N_{v3B} number was 2.08, CMSX-10B was designed to the 2.02 level. This was accomplished by the further reduction of alloy Cr content and similar reduction to Co and W+Re level. W was reduced more than the Re in this specimen since Re is more effective in the solid solution. Additionally, wherein some loss in W contribution to the gamma prime could be anticipated, it was sufficiently replaced by the modest increase to Ta content in this composition. These changes resulted in the CMSX-10B alloy specimen exhibiting even more improved creep strength at 1800° F. Table 6 reported below illustrates that three specimens achieved an average life of 961 hours, with 1.0% creep occurring at an average of 724 hours. However, it was observed that TCP phase was present at higher temperature.

TABLE 6

CMSX-10B CREEP-RUPTURE

TEST CONDITION	RUPTURE TIME HOURS	% ELONG.	% RA	FINAL CREEP READING t, hours	FINAL CREEP READING % deformation	TIME IN HOURS TO REACH 1.0%	TIME IN HOURS TO REACH 2.0%
1800° F./36.0 ksi	907.1	19.2	34.0	907.0	17.832	697.2	752.7
	989.3	18.9	33.5	988.5	17.657	768.1	817.8
	988.4	35.9	36.1	987.3	31.813	705.8	767.5
	507.0	44.1	45.4	505.7	41.548	317.9	352.6
	598.1	46.9	43.4	596.1	42.340	386.5	415.2

TABLE 6-continued

TEST CONDITION	RUPTURE TIME HOURS	% ELONG.	% RA	FINAL CREEP READING t, hours	FINAL CREEP READING % deformation	TIME IN HOURS TO REACH 1.0%	TIME IN HOURS TO REACH 2.0%
	CMSX-10B CREEP-RUPTURE						
	408.3	62.6	52.1	407.2	54.479	187.3	256.5
	265.3	39.7	43.7	262.7	37.102	87.6	119.2
	385.3	45.5	46.2	383.5	39.031	177.4	213.4
	412.8	43.4	40.5	410.6	38.771	189.1	233.4
	389.3	51.5	44.2	386.8	36.920	220.5	249.2
	459.5	40.0	46.3	458.0	39.513	210.2	291.1
	258.0	38.1	40.6	257.9	36.743	32.1	90.2
	484.1	27.9	40.0	483.4	26.296	288.1	326.7
	376.9	16.4	20.4	376.8	16.088	96.0	226.6
	481.0	50.5	48.2	478.8	34.557	264.4	297.5
	461.5	35.1	40.6	460.1	30.786	181.1	265.3
	483.0	47.1	46.8	482.1	43.714	286.2	320.7
	500.1	33.4	37.0	499.7	30.486	11.9	280.1
1800° F./40 ksi	436.7	40.2	44.1	436.2	39.818	294.6	318.9
	390.8	50.1	42.8	390.3	41.817	250.9	276.2
	336.9	52.7	48.1	335.2	46.697	226.5	240.9
1900° F./25.0 ksi	237.8	55.9	45.7	237.4	53.854	33.0	113.5
	295.7	57.4	49.1	295.6	46.592	123.7	170.9
2000° F./18.0 ksi	192.7	31.5	26.6	191.6	27.733	56.3	88.6
	166.5	41.4	25.3	166.5	34.102	46.2	72.7
	173.3	36.6	27.0	171.4	31.481	24.0	66.1
2050° F./15.0 ksi	219.6	40.1	40.4	218.6	37.871	13.2	56.8
	122.3	28.2	47.9	120.6	26.614	37.0	63.7
	118.4	33.2	60.0	116.9	29.986	36.7	56.5
	179.7	44.1	48.1	179.1	39.188	8.4	75.3
	74.9	44.2	48.6	74.6	34.800	6.8	14.5
	168.3	48.6	49.7	167.0	43.171	36.9	77.1
	104.8	17.0	27.2	102.8	1.626	66.1	—
	155.9	46.3	49.8	155.2	38.388	64.4	81.9
	90.6	15.1	21.4	87.1	1.046	75.5	—
	120.5	46.3	55.8	118.7	35.143	10.3	27.7
	150.7	39.8	49.7	150.1	33.903	21.4	60.9
	149.5	33.2	46.2	148.9	23.166	73.3	88.3
	142.9	42.0	47.5	142.5	41.524	54.9	70.5
2050° F./15.0 ksi	163.0	52.5	49.2	161.9	46.146	20.5	76.9
	151.1	66.4	45.6	150.7	59.115	52.7	75.5
	131.8	57.3	44.4	131.5	48.310	26.3	57.1
	*156.0	54.4	41.0	155.9	45.502	55.5	78.3
	*133.7	57.2	56.0	132.7	41.753	67.5	80.7
	*135.1	59.7	52.3	134.3	46.317	54.9	71.5
	151.1	66.4	45.6	150.7	59.115	52.7	75.5
	131.8	57.3	44.4	131.5	48.310	26.3	57.1
2100° F./15.0 ksi	69.7	54.2	48.1	69.4	47.674	25.3	36.3

*As-Solutioned Condition

Only about 97–98% gamma prime solutioning was achieved in the CMSX-10A and -10B materials (see Table 4) which was insufficient for the purpose of optimizing alloy mechanical properties and microstructural homogeneity. Attainment of a greater level of gamma prime solutioning, therefore, became an equal priority in tandem with improving microstructural stability at temperatures above 1900° F.

To confirm the suspected composition of the TCP phase forming in the alloys, scanning electron microscope (SEM) wavelength dispersive x-ray (WDX) microchemistry analyses of CMSX-10B test bar contained needles was undertaken and compared to the alloys gamma and gamma prime compositions. The results, reported in Table 7 below, confirm that the needles were enriched in Cr, W and Re.

TABLE 7

CMSX-10B Micro-Chemistry Analyses
Cast Test Bar (VF 831)
Transverse Section. Bottom Bar Location.
Solutioned to 2465° F.
Aged 1975° F./19.5 Hrs./AC
1600° F./20 Hrs./AC
1400° F./24 Hrs./AC

ELEM	GAMMA PHASE K	GAMMA PHASE Z	GAMMA PHASE A	GAMMA PHASE F	GAMMA PRIME PHASE K	GAMMA PRIME PHASE Z	GAMMA PRIME PHASE A	GAMMA PRIME PHASE F	NEEDLE CONSTITUENT K	NEEDLE CONSTITUENT Z	NEEDLE CONSTITUENT A	NEEDLE CONSTITUENT F
ALK	0.0101	1.090	0.324	1.000	0.0145	1.084	0.322	1.000	0.0116	1.107	0.347	1.000
TIK	0.0069	1.007	0.930	1.051	0.0084	1.002	0.934	1.052	0.0077	1.026	0.908	1.039
CRK	0.0428	1.008	0.963	1.108	0.0250	1.002	0.965	1.117	0.0390	1.028	0.949	1.083
COK	0.0970	0.994	0.984	1.018	0.0761	0.988	0.987	1.022	0.0755	1.016	0.977	1.025
NIK	0.6891	1.033	0.988	1.010	0.7270	1.026	0.991	1.005	0.6143	1.056	0.983	1.024
TAL	0.0485	0.794	1.020	1.000	0.0697	0.788	1.024	1.000	0.0389	0.814	1.018	1.000
W L	0.0329	0.788	0.963	1.000	0.0311	0.783	0.962	1.000	0.0682	0.808	0.968	1.000

TABLE 7-continued

REL	0.0422	0.785	0.968	1.000	0.0085	0.779	0.968	1.000	0.1083	0.805	0.973	1.000
						WT %			WT %			WT %
				ELEM	CPS	ELEM	CPS		ELEM	CPS		ELEM
				AL K	12.1800	2.87	17.9400		4.19	11.9900		3.02
				TI K	5.5200	0.71	6.8400		0.86	5.2500		0.79
				CR K	27.6400	3.98	16.4500		2.31	21.5800		3.69
				CO K	40.6800	9.74	32.5400		7.64	27.1700		7.42
				NI K	253.1300	66.84	272.3800		71.11	193.7500		57.84
				TA L	6.5667	5.99	9.6329		8.64	4.5259		4.70
				W L	4.0775	4.33	3.9375		4.13	7.2620		8.71
				RE L	4.6000	5.56	0.9500		1.13	10.1300		13.82
				TOTAL		100.00			100.00			100.00

The calculated N_{v3B} numbers were 1.90 for CMSX-10C and 1.95 for CMSX-10D. Re was maintained at around 5% while W was further reduced to improve stability in these specimens. Alloy Ta was increased since it did not participate in TCP formation and the Ta/W ratio was effectively improved, which assisted with alloy castability. Chromium was reduced in the -10C specimens but increased to 4.0% in the -10D specimens to provide an opportunity to determine the suitability of the Cr levels from a hot corrosion standpoint. Co was reduced in both materials, significantly in the -10D specimen, while Ai+Ti level was also reduced to assist in achieving more complete gamma prime solutioning. Creep-rupture results for the two specimens are reported below in Tables 8 and 9, respectively. Even though the -10D alloy specimens were observed to exhibit full gamma prime solutioning (as opposed to 99.-99.5% for CMSX-10C) the alloys greater Cr content, which necessitated a lower Ai+Ti level, effected lower properties than attained with CMSX-10C. However, both materials exhibited improved alloy stability and higher temperature properties, so that attempts to balance the alloys low and high temperature creep response were favorable.

TABLE 8

CMSX-10C CREEP-RUPTURE

TEST CONDITION	RUPTURE TIME HOURS	% ELONG.	% RA	FINAL CREEP READING t, hours	FINAL CREEP READING % deformation	TIME IN HOURS TO REACH 1.0%	TIME IN HOURS TO REACH 2.0%
1800° F./36.0 ksi	556.1	31.4	30.5	555.2	26.615	316.1	376.3
	636.6	43.9	37.5	636.4	38.460	416.6	455.4
	609.2	23.3	34.7	607.6	19.074	410.6	460.6
	635.7	44.9	45.6	635.3	34.991	407.3	443.4
	612.8	43.5	38.8	611.9	41.951	409.8	438.7
1850° F./36.0 ksi	252.2	30.2	37.8	252.0	22.033	61.1	166.3
	298.1	41.3	39.0	297.6	37.953	170.3	194.8
	231.1	33.6	39.5	230.2	29.689	127.8	146.0
1922° F./20.3 ksi	492.4	52.5	52.4	491.6	48.922	176.5	251.7
	529.8	38.6	45.5	528.9	33.353	269.6	306.2
	637.5	48.9	43.3	635.2	45.804	189.5	318.3
2000° F./18.0 ksi	258.8	35.0	41.5	258.7	32.444	74.2	127.5
	293.1	49.2	44.1	292.1	42.079	145.6	170.9
	221.9	43.0	48.5	220.9	33.507	55.6	123.3
	266.1	35.1	44.0	264.6	33.759	113.6	143.6
2050° F./15.0 ksi	196.6	39.7	40.3	194.1	27.755	26.0	134.8
	170.4	30.1	46.3	169.2	25.624	11.1	51.4
	193.2	38.1	42.9	191.9	32.288	46.5	76.5
	247.3	33.1	40.5	246.0	26.494	122.0	150.8

TABLE 9

CMSX-10D CREEP-RUPTURE

TEST CONDITION	RUPTURE TIME HOURS	% ELONG.	% RA	FINAL CREEP READING t, hours	FINAL CREEP READING % deformation	TIME IN HOURS TO REACH 1.0%	TIME IN HOURS TO REACH 2.0%
1800° F./36.0 ksi	428.0	26.7	29.3	426.3	24.166	189.2	248.3
1850° F./36.0 ksi	141.0	23.1	26.8	140.1	20.660	57.8	79.7
	140.7	14.7	26.1	140.2	13.741	56.2	77.6
	166.0	17.5	28.9	165.0	15.640	76.5	100.1
1922° F./20.3 ksi	519.9	23.8	24.9	518.9	22.608	202.0	345.6
	667.0	17.6	23.7	665.2	16.819	151.8	391.4
	680.3	14.9	28.2	678.9	14.476	340.2	500.3
2000° F./18.0 ksi	370.3	18.8	21.3	369.9	15.560	20.9	106.9
	401.5	11.1	18.0	400.0	8.903	19.8	125.5
	366.6	17.5	25.8	366.6	8.049	223.9	306.1
2050° F./15.0 ksi	465.3	12.9	20.5	465.2	12.639	61.0	305.9
	338.8	9.8	24.8	337.7	9.468	30.8	204.4

The acceptability of the alloys' low Cr content was confirmed through extremely aggressive short-term burner rig hot corrosion tests performed at 1650° F., 1% sulfur, 10 ppm sea salt condition. FIGS. **1** and **2** illustrate the results for tests performed to 117 and 144 hours for the CMSX-10C and CMSX-10D specimens, respec-

tively. In both cases, the materials performed similar to MAR M 247-type materials, thereby confirming the suitability of the low Cr alloy design concept.

With the above-noted results, another series of alloys, CMSX-10E, -10F, -10G, -10H, -10I,and -12A were designed, produced and evaluated. The alloys explored Re level ranging 4.8–6.3%, 2.2–3.0% Cr level, 4.7–7.6% Co level and the remainder balanced to maintain castability, improve solutionability and improve phasial stability. The N_{v3B} number ranged between 1.81–1.89.

One of the series, CMSX-10F, contained 0.02% C and 0.02% B. These additions were observed to improve casting yield and may have assisted in providing more consistent control of single crystal cast article orientation. However, the melting point depressants, C and B, restricted the specimen's response to solution heat treatment. The CMSX-10F creep-rupture properties are reported in Table 10 below.

TABLE 10

CMSX-10F CREEP-RUPTURE

TEST CONDITION	RUPTURE TIME HOURS	% ELONG.	% RA	FINAL CREEP READING t, hours	FINAL CREEP READING % deformation	TIME IN HOURS TO REACH 1.0%	TIME IN HOURS TO REACH 2.0%
1800° F./36.0 ksi	616.0	18.1	22.4	615.8	16.898	439.9	477.6
	666.6	45.6	48.0	666.4	43.261	464.6	492.3
	603.1	25.3	24.3	602.5	24.281	398.4	444.0
1850° F./36.0 ksi	243.9	19.6	28.2	243.0	18.045	129.1	160.9
	285.9	26.8	32.1	285.5	25.701	187.8	206.0
	258.6	19.2	29.1	258.3	18.175	168.3	189.5
1922° F./20.3 ksi	499.5	40.0	41.0	498.5	37.756	208.2	272.6
	649.2	55.6	52.9	648.3	51.045	197.6	338.8
	361.0	15.8	21.9	357.7	2.599	273.2	335.7
2000° F./18.0 ksi	235.4	39.6	51.7	235.4	37.881	100.8	133.2
	276.1	43.7	52.8	274.4	36.762	115.1	155.9
	290.0	36.7	47.3	289.1	33.304	125.3	162.1
2050° F./15.0 ksi	255.4	28.7	36.6	255.0	27.426	67.4	131.0
	255.1	33.4	43.1	254.9	31.378	46.2	102.2
	254.5	25.4	33.3	254.4	23.737	50.9	118.7

The CMSX-10E, G, H and I, plus CMSX-12A creep-rupture specimen results are reported below in Tables 11, 12, 13, 14, and 15, respectively. The results show a general improvement to alloy creep-rupture strength above 1900° F. while maintaining extremely good strength at lower temperatures.

TABLE 11

CMSX-10E CREEP-RUPTURE

TEST CONDITION	RUPTURE TIME HOURS	% ELONG.	% RA	FINAL CREEP READING t, hours	FINAL CREEP READING % deformation	TIME IN HOURS TO REACH 1.0%	TIME IN HOURS TO REACH 2.0%
1800° F./36.0 ksi	664.5	31.4	36.3	663.5	30.435	436.5	470.8
	604.4	35.1	36.7	603.3	33.371	253.7	355.9
	582.5	41.5	36.1	581.7	39.792	78.9	329.3
	553.5	35.9	37.0	552.5	33.172	326.4	357.1
1850° F./36.0 ksi	257.9	25.3	32.0	257.0	22.734	149.4	170.3
	199.2	18.4	32.1	198.6	16.261	122.4	139.4
	260.5	33.6	33.4	259.7	31.315	159.9	174.0
1922° F./20.3 ksi	810.6	38.6	33.0	808.4	33.523	210.2	378.2
	800.9	35.3	36.4	799.1	32.405	339.7	434.2
	859.9	39.0	35.4	859.6	37.036	364.6	465.2
2000° F./18.0 ksi	362.8	27.7	29.3	362.4	24.887	98.4	177.3
	411.2	29.4	27.0	409.9	26.426	173.6	218.6
	369.7	15.3	28.2	368.8	12.941	170.3	221.9
	379.7	26.4	26.1	379.2	27.656	177.9	206.6
2050° F./15.0 ksi	476.9	21.8	23.4	476.3	18.233	196.6	255.9
	418.4	27.5	24.7	417.5	25.854	180.0	227.3
	397.7	19.0	23.8	396.8	17.522	112.6	198.2

TABLE 12

CMSX-10G CREEP-RUPTURE

TEST CONDITION	RUPTURE TIME HOURS	% ELONG.	% RA	FINAL CREEP READING t, hours	FINAL CREEP READING % deformation	TIME IN HOURS TO REACH 1.0%	TIME IN HOURS TO REACH 2.0%
1700° F./55.0 ksi	671.8	19.6	28.6	670.5	14.775	447.2	508.1
	693.6	26.0	24.2	691.7	21.750	441.2	493.4
	724.9	23.3	29.7	723.2	19.913	464.8	520.4
	582.5	18.6	20.1	581.1	15.200	77.0	356.7
	681.2	20.9	24.1	679.2	19.115	56.4	314.8
	538.4	21.6	17.5	538.3	17.857	242.1	308.7
	523.0	17.7	21.8	522.4	14.157	235.3	308.0
	569.7	17.5	19.8	568.5	15.035	287.0	354.9
1800° F./36.0 ksi	775.2	29.6	29.3	773.8	28.826	315.0	539.9
	719.7	29.5	28.5	717.8	27.266	321.2	486.4
	741.6	28.0	25.9	740.3	24.870	284.5	464.2
	682.8	45.6	34.7	681.1	39.289	409.1	452.4

TABLE 12-continued

CMSX-10G CREEP-RUPTURE

TEST CONDITION	RUPTURE TIME HOURS	% ELONG.	% RA	FINAL CREEP READING t, hours	FINAL CREEP READING % deformation	TIME IN HOURS TO REACH 1.0%	TIME IN HOURS TO REACH 2.0%
	764.0	23.2	33.7	764.0	22.884	543.6	586.6
	790.4	41.4	35.6	789.4	38.172	511.6	565.3
	799.1	27.0	32.3	797.4	25.737	529.8	579.1
1850° F./36.0 ksi	354.4	19.3	30.2	351.9	16.000	246.7	271.4
	344.5	28.5	31.9	344.3	26.174	220.8	241.9
	315.4	23.7	30.7	315.1	23.571	183.4	205.6
1922° F./20.3 ksi	753.4	31.7	34.8	753.2	27.914	352.3	462.1
	728.0	31.5	33.5	727.1	28.362	281.1	422.1
	731.6	34.3	38.8	730.5	30.770	339.3	437.3
1976° F./28.1 ksi	95.4	29.3	29.4	94.9	22.842	41.5	50.9
	95.7	26.7	27.2	94.7	20.130	45.8	54.7
	104.6	30.4	33.2	104.4	27.517	41.8	54.4
	100.8	25.6	35.1	98.9	21.577	49.2	58.1
	95.8	25.9	28.9	93.6	19.748	41.1	51.4
	110.0	29.3	30.3	108.0	22.669	48.5	60.1
	108.2					43.8	
	104.8					45.8	
	104.3					48.6	
2000° F./18.0 ksi	464.4	23.1	21.3	463.6	18.190	257.7	293.5
	411.9	18.3	23.0	410.4	16.347	103.5	227.6
	370.9	27.0	38.7	369.8	25.326	7.6	47.3
2012° F./14.5 ksi	790.2	31.2	34.9	788.7	24.939	299.9	406.0
	671.4	23.6	25.7	670.3	13.397	303.3	396.3
	512.1	22.6	28.1	510.4	21.094	192.5	277.7
	651.7	27.4	39.7	651.3	16.328	315.7	434.7
	754.6	29.7	25.4	753.1	24.032	193.8	388.7
	908.3	17.7	18.3	—	—	—	—
	758.9	30.8	26.5	758.7	24.090	388.7	438.2
	740.0	19.8	20.5	739.5	16.962	316.5	426.7
	671.5	26.4	23.8	669.3	15.578	359.8	412.4
2050° F./15.0 ksi	410.8	22.9	27.4	410.0	18.655	226.5	272.2
	283.5	18.0	31.2	283.5	15.303	156.4	191.2
	320.0	16.8	17.4	318.3	12.979	156.4	191.2
	389.7	22.0	22.1	389.7	18.488	29.9	189.1
	381.4	27.0	24.1	381.1	24.758	69.5	197.9
2100° F./12.0 ksi	254.4	12.7	30.4	252.9	8.984	108.4	185.5
	419.8	20.5	26.0	419.8	18.917	201.1	274.3
2100° F./12.5 ksi	331.4	16.9	21.7	331.1	15.069	25.2	83.2
	367.7	19.2	23.2	366.5	17.530	76.2	177.4
	387.3	16.8	17.2	386.5	12.742	236.9	282.0
	383.1	34.1	32.4	381.6	32.135	10.5	164.3

TABLE 13

CMSX-10H CREEP-RUPTURE

TEST CONDITION	RUPTURE TIME HOURS	% ELONG.	% RA	FINAL CREEP READING t, hours	FINAL CREEP READING % deformation	TIME IN HOURS TO REACH 1.0%	TIME IN HOURS TO REACH 2.0%
1800° F./36.0 ksi	563.4	23.2	27.2	563.2	22.669	318.5	366.2
	553.1	24.5	23.0	552.7	21.324	373.1	402.8
	526.9	20.7	27.3	526.4	19.715	358.2	390.7
	594.5	35.1	41.4	594.4	32.090	328.8	372.8
1850° F./36.0 ksi	242.9	24.3	20.1	242.2	20.686	107.3	155.6
	221.9	17.0	21.0	221.0	14.888	115.9	150.4
	223.4	21.3	21.0	221.7	19.196	128.4	144.7
1922° F./20.3 ksi	520.6	26.1	29.3	520.4	23.183	234.3	319.1
	470.4	26.3	21.2	469.2	19.333	176.1	253.2
	574.7	16.8	23.0	573.0	14.411	282.1	373.0
2000° F./18.0 ksi	434.0	21.5	18.7	432.1	20.234	103.5	233.1
	437.3	27.1	33.8	437.3	26.306	182.6	240.8
	430.7	24.6	20.4	430.7	23.244	68.8	192.1
	430.1	21.1	19.3	428.9	19.050	73.7	213.8
2050° F./15.0 ksi	366.1	16.3	12.0	365.5	11.326	239.8	273.3
	384.0	17.4	16.0	382.3	12.055	168.2	242.9
	420.2	12.2/ 13.3	418.6	10.017	127.3	273.2	

TABLE 14

CMSX-10 I CREEP-RUPTURE

TEST CONDITION	RUPTURE TIME HOURS	% ELONG.	% RA	FINAL CREEP READING t, hours	FINAL CREEP READING % deformation	TIME IN HOURS TO REACH 1.0%	TIME IN HOURS TO REACH 2.0%
1800° F./36.0 ksi	565.1	35.2	32.0	564.8	29.774	297.0	368.9

TABLE 14-continued

CMSX-10 I CREEP-RUPTURE							
	RUPTURE TIME	%	%	FINAL CREEP READING		TIME IN HOURS TO REACH	
TEST CONDITION	HOURS	ELONG.	RA	t, hours	% deformation	1.0%	2.0%
	581.9	32.4	29.3	580.2	28.689	371.9	402.5
	514.1	24.1	30.2	514.1	21.207	318.3	358.2
1850/36.0	260.5	25.0	24.8	259.3	23.255	156.7	175.3
	247.5	22.4	29.1	245.7	17.730	131.9	169.0
	246.1	23.7	29.0	246.1	20.277	137.6	156.7
1922/20.3	916.3	24.9	30.3	914.8	22.465	472.9	549.3
	934.8	32.2	33.0	934.8	30.165	353.7	475.2
	863.6	27.8	28.5	862.9	27.057	295.6	442.5
1976/28.1	116.1	19.5	20.1	116.1	19.155	57.4	70.1
	65.6	22.9	20.6	64.2	21.368	17.8	26.4
	91.6	23.2	25.3	90.4	15.544	37.6	49.7
2000/18.0	430.1	22.7	25.7	429.2	18.449	58.9	193.0
	483.8	19.8	25.1	483.8	17.860	102.4	245.4
2050/15.0	397.7	17.9	30.0	397.3	13.264	239.8	292.9
	487.7	21.4	21.9	487.1	18.854	248.2	318.4
	468.3	18.4	25.5	467.9	15.800	194.1	300.1
2100/12.0	501.3	10.1	15.9	498.7	0.615	—	—
	401.3	16.8	26.3	399.7	15.429	6.6	25.5
	210.6	11.5	12.7	210.3	0.373	—	—

TABLE 15

CMSX-12A CREEP-RUPTURE							
	RUPTURE TIME	%	%	FINAL CREEP READING		TIME IN HOURS TO REACH	
TEST CONDITION	HOURS	ELONG.	RA	t, hours	% deformation	1.0%	2.0%
1800° F./36.0 ksi	491.9	40.2	41.6	491.8	38.605	254.0	293.7
	420.4	23.5	31.9	420.3	19.299	234.9	277.9
	383.4	25.3	26.2	382.9	22.920	198.1	244.3
	456.2	24.1	26.1	454.5	22.582	89.9	265.5
	458.0	30.7	32.7	457.1	26.155	253.2	292.8
	386.8	30.1	30.4	386.3	27.031	172.7	216.9
	403.7	34.5	28.8	402.7	31.033	140.2	204.9
	398.7	21.6	23.5	398.4	20.277	181.1	236.1
1850/36.0	208.5	32.1	40.5	208.3	31.248	100.8	119.6
	189.5	21.2	25.2	189.4	20.461	99.1	116.3
1922/20.3	829.6	46.5	45.3	828.8	44.488	315.8	400.7
	797.0	33.5	32.5	796.9	32.856	315.3	400.5
2000/18.0	500.3	31.7	29.6	499.2	24.922	218.4	268.5
	227.6	36.5	41.2	227.1	26.825	90.6	113.9
	430.4	18.5	23.3	430.4	18.180	181.0	234.1
2050/15.0	424.8	17.0	27.5	423.3	15.832	263.5	301.2
	366.1	26.2	42.8	365.5	20.399	146.6	197.8
	400.8	18.2	25.4	400.7	16.910	184.6	251.3
2100/12.0	255.4	25.8	45.8	253.6	22.920	64.1	125.8
	483.9	10.1	19.3	482.7	8.602	378.6	421.9
	325.1	7.1	16.6	324.7	4.315	268.8	302.5

Varying the primary gamma prime aging treatment was explored with most of the development activity concentrated on achieving optimized gamma prime size and distribution through longer soak times at 1975° F. (see Table 4) since higher temperature aging treatments accelerated TCP phase formation during the aging cycle.

Ten to twenty-one hour soak times at 1975° F. were successful since they provided average gamma prime particles of about 0.5 um dimension. However, it appeared that shorter primary gamma prime aging time at higher temperature may be more practical, once more stable microstructures were defined.

Microchemical SEM WDX needle particle analyses was performed on a failed CMSX-10G creep-rupture specimen. The specimen, tested at 1976° F./28.1 ksi condition, exhibited needles in its microstructure. The results of the analysis are reported in Table 16 below and indicate, again, that the needles formed in this class of material are particularly rich in Re, but are also enrichened with Cr and W.

TABLE 16

CMSX-10G
1976° F./28.1 ksi
104.6 HRS.

ELEM	K	Z	A	F
CRK	0.0426	1.105	0.793	1.049
COK	0.0584	1.094	0.888	1.086
NIK	0.1740	1.140	0.910	1.116
W L	0.2107	0.941	0.972	1.000
REL	0.4767	0.941	0.979	1.000

NEEDLE CHEMISTRY

ELEM	CPS	WT % ELEM
CRK	113.7000	4.63
COK	112.1100	5.54
NIK	305.1425	15.02
W L	134.8988	23.03
REL	276.4000	51.76
		100.00

A standardized test for resistance to recrystallization was performed on a CMSX-10G test bar. The test

method and the results are reported in Table 17 below. The test results indicate that the CMSX-10G specimen exhibited similar resistance to cast process/solution treatment/bonding process recrystallization level in comparison to CMSX-4 alloy.

TABLE 17

•Method: A controlled level of compressive stress is imparted on the entire surface of an as-cast test bar. The bar is then solution heat treated. Following solution treatment, the bar is sectioned and the transverse section is observed metallographically. Depth of recrystallization measurements are taken.

•Evaluation Standards:

Alloy	Depth of RX	Resistance to RX Anticipated in Blade Castings
CMSX-4	.004"	Very Good
SX 792	Entire Bar	Very Poor
CMSX-10G	.004"	Very Good

The CMSX-10Ga -10Ia, -12B,-12C, -10J, -10Ri and -12Ri compositions were defined and evaluated. No creep-rupture properties were generated for the CMSX-10J specimen, although test bars were produced and a solution heat treatment developed. Again, the inclusion of C and B in the -10J composition appeared to have positive effect to single crystal test specimen yield. Additionally, the lower levels of C and B than evaluated in CMSX-10F specimen, particularly lower B, made the material more amenable to solution heat treatment. Ninety-eight to ninety-nine percent gamma prime solutioning was achieved, as opposed to the approximate 95% level typical of the CMSX-10F composition.

The CMSX-10Ga and -10Ia alloys were designed with N_{v3B} numbers of about 1.70. These alloy specimens contain about 2.5% Cr, 3.3–4.0% Co, 5.6–6.0% Re, greater Ta/W ratio, reduced Cb, and reduced Ai+Ti content. Such reduction to Cb+AI+Ti level improved the solutioning characteristics of the materials (see Table 4), plus assisted achievement of increased alloy stability. Both specimens exhibited nearly full gamma prime solutioning.

The lowered N_{v3B} number continued to show effectiveness in providing better creep-rupture capability at temperature greater than 1900° F., while maintaining extremely good creep-strength at lower temperature. CMSX-10Ga test results from specimens produced with improved casting process controls exhibited 700 hours or more life with about 475 hours required to creep to 1.0% for 1800° F./36.0 ksi condition. For higher temperature exposure, the specimen provided the improved average life of about 500 hours at 2050° F./15.0 ksi condition and average 1.0% creep deformation that occurred at about 250 hours, as indicated by the results reported in Table 18 below.

TABLE 18

CMSX-10Ga CREEP-RUPTURE

TEST CONDITION	RUPTURE TIME HOURS	% ELONG.	% RA	FINAL CREEP READING t, hours	FINAL CREEP READING % deformation	TIME IN HOURS TO REACH 1.0%	TIME IN HOURS TO REACH 2.0%
1800° F./36.0 ksi	500.7	19.9	25.2	499.7	19.541	316.5	360.1
	584.2	29.1	25.4	583.9	26.395	370.0	401.8
	505.1	22.6	29.8	503.7	18.212	307.4	347.3
	730.9	42.0	42.8	730.7	40.216	477.6	516.1
						460.6	
						428.5	
1850/36.0	184.5	41.0	33.9	183.2	37.154	82.3	94.5
	291.5	27.3	29.9	290.2	19.323	191.6	207.8
	279.5	33.9	32.5	278.1	29.054	155.3	180.5
	323.9	30.9	36.6	322.9	29.218	194.1	217.1
	326.5+	8.9	12.6	—	—	—	—
	295.2+	33.3	33.5	—	—	—	—
						174.1	
						162.3	
	300.1+	22.8	22.4	—	—	—	—
1976/28.1	88.6	34.9	33.9	88.6	25.502	39.7	48.9
	100.1	28.2	29.2	98.8	19.706	53.9	61.3
	107.9	28.8	31.4	107.0	23.657	51.1	62.1
	87.1	27.0	33.8	87.1	24.177	39.2	48.5
	82.8	23.3	27.7	81.0	17.301	20.6	38.0
	88.2	31.2	35.2	86.4	24.463	33.6	44.4
	83.7	34.0	34.3	83.4	29.718	36.3	45.1
	114.1	24.3	26.3	113.0	20.544	62.1	73.2
	122.3	18.3	21.3	120.7	15.740	76.5	86.0
	117.7	23.2	25.6	117.5	22.284	78.0	85.3
	(INTERRUPTED TESTS)			40.2	1.036	39.9	—
				43.4	1.187	42.3	—
	99.3+	60.1	38.8	—	—	—	—
	127.9	41.5	34.5	127.5	37.493	51.2	62.6
	96.8	22.9	27.9	96.5	20.124	45.9	54.4
	118.9	31.3	27.1	118.0	24.603	49.5	61.3
	111.1	25.0	22.8	110.2	21.521	46.4	58.0
	96.6+	24.1	22.9	—	—	—	—
	120.5+	25.8	29.4	—	—	—	—
	113.0+	27.6	20.5	—	—	—	—
1976/18.85	(INTERRUPTED TESTS)			261.5	1.015	260.3	—
				207.2	1.017	204.6	—
	592.1	25.8	22.4	590.4	23.596	210.1	305.9
	570.7	27.2	26.9	570.7	26.289	293.3	332.6
	535.5	19.3	23.9	535.2	17.513	308.2	344.2
						240.5	
						307.6	

TABLE 18-continued

CMSX-10Ga CREEP-RUPTURE							
				FINAL CREEP READING		TIME IN HOURS TO REACH	
TEST CONDITION	RUPTURE TIME HOURS	% ELONG.	% RA	t, hours	% deformation	1.0%	2.0%
2050/15.0	536.8	28.5	27.5	535.6	20.662	232.3	321.3
	497.0	23.7	23.9	496.2	17.600	260.3	317.9
	514.8	23.4	24.4	513.1	12.500	230.4	340.4
	454.1	16.6	35.2	453.7	15.476	263.2	317.1
	420.3+	33.7	33.2	—	—	—	—
	(INTERRUPTED TESTS)		—	—	—	239.1	—
			—	—	—	189.6	—
			—	—	—	280.3	—
	560.1+	—	22.9	—	—	—	—
2012/14.5	536.6+	7.3	8.1	—	—	—	—
						424.6	
2100/12.0	354.1	14.8	36.5	353.8	12.646	91.2	219.1
	343.4+	—	27.2	—	—	—	—
						91.4	
						147.2	
	491.0+	—	16.7	—	—	—	—
1700/50.0	+						

+Machined From Blade Specimen

1% creep strength is a significant property. Limiting creep strains to 1.0% and 2.0% is extremely important to gas turbine component design, since a component's usefulness is generally measured by its resistance to creep to an approximate 1-2% level, not its ultimate rupture strength. Many prior art alloys may exhibit attractive rupture strength at the >1900° F. level, however, they lack the level of useful strength, i.e., creep strength to 2.0%, that this invention provides in tandem with its far superior strength in test conditions below 1900° F.

The CMSX-10Ia specimens also provided significantly increased creep strength at the higher temperature extremes, but it did not appear to develop strength as good as the CMSX-10Ga specimens in lower temperature tests, as indicated by the results in Table 19 below.

TABLE 19

CMSX-10 Ia CREEP-RUPTURE							
				FINAL CREEP READING		TIME IN HOURS TO REACH	
TEST CONDITION	RUPTURE TIME HOURS	% ELONG.	% RA	t, hours	% deformation	1.0%	2.0%
1800° F./36.0 ksi	532.0	34.8	32.7	530.7	33.000	259.1	312.5
	474.6	23.8	29.2	473.1	22.886	201.0	269.2
	374.3	20.0	21.0	372.8	19.238	171.1	214.7
1850/36.0	256.0	28.7	28.5	256.0	27.867	135.4	157.1
	251.4	34.4	30.3	250.7	33.055	121.6	144.6
	217.8	30.5	22.4	217.2	27.000	94.2	117.9
1976/28.1	85.7	27.5	28.9	83.8	21.754	36.9	46.2
	81.9	33.6	31.8	81.0	24.384	32.1	42.1
	68.9	26.1	25.8	67.6	20.960	23.1	32.4
2012/14.5	930.2	10.0	14.4	928.4	9.649	104.6	455.7
	844.4	17.7	23.2	842.8	16.132	339.7	502.3
	864.2	15.3	11.9	862.8	14.558	179.9	453.4
2050/15.0	510.2	17.8	19.7	508.4	15.703	187.2	312.7
	528.6	17.9	24.2	527.0	14.873	293.7	364.3
	438.8	14.3	11.3	436.4	13.556	56.0	136.9
2100/12.0	616.4	19.0	19.1	616.3	14.112	60.0	422.5
	467.7	19.1	26.1	466.0	11.373	273.6	374.8

Similarly, CMSX-12B, with Nv3B at 1.80 level and additional chemistry balance as presented in Table 1, provided attractive creep strength at test condition greater than 1900° F., but did not perform quite as well as CMSX-10Ga in lower temperature tests, as indicated by the results reported in Table 20 below.

TABLE 20

CMSX-12B CREEP-RUPTURE							
				FINAL CREEP READING		TIME IN HOURS TO REACH	
TEST CONDITION	RUPTURE TIME HOURS	% ELONG.	% RA	t, hours	% deformation	1.0%	2.0%
1976° F./28.1 ksi	91.7	15.3	17.2	91.2	14.070	43.9	56.2
	72.6	19.4	23.2	72.6	17.396	27.4	36.8
	14.1	5.0	1.3	12.7	2.300	8.6	11.9
	98.1	16.9	17.6	96.4	13.670	17.8	38.9
	108.2	25.2	24.1	108.0	22.794	43.8	58.7
	106.9	24.7	24.2	106.3	21.024	46.1	60.1
	104.8	24.0	26.8	104.3	20.094	45.8	58.7
	104.3	26.8	21.4	103.2	22.347	48.6	60.8
1800/36.0	515.0	24.7	24.2	513.3	19.468	320.1	358.0

TABLE 20-continued

CMSX-12B CREEP-RUPTURE							
	RUPTURE TIME	%	%	FINAL CREEP READING		TIME IN HOURS TO REACH	
TEST CONDITION	HOURS	ELONG.	RA	t, hours	% deformation	1.0%	2.0%
	536.4	23.2	21.1	530.8	22.184	318.3	359.5
	304.7	13.2	19.9	302.9	12.582	166.0	200.8
1850/36.0	262.6	18.4	23.1	262.4	17.660	12.5	142.2
2012/14.5	1031.3	17.2	18.5	1029.5	15.113	428.0	703.7
	1078.7	15.6	20.0	1076.7	15.217	704.2	819.2
	839.4	14.9	22.8	839.2	9.282	607.6	677.7
	836.9	23.2	21.0	834.8	18.024	591.1	658.5
	722.0	16.4	21.1	721.9	15.913	170.8	333.6
	711.3	14.5	18.8	710.8	12.490	381.9	531.5
	711.9	18.3	20.0	711.4	16.201	447.7	530.7
2050/15.0	507.5	10.0	10.1	507.2	9.394	70.4	360.4
	434.0	17.5	16.8	434.0	13.847	241.7	309.0
2100/12.0	487.5	25.3	20.3	486.6	20.986	18.2	224.7
	444.9	7.8	11.0	442.2	3.884	347.3	413.6

Alloy composition has the greatest effect on ultimate creep strength. However, some of the variation experienced between alloy derivatives, and particularly for tests exhibiting inconsistent results for a given alloy, can be caused by variation in casting process condition. Casting process thermal gradient variation affects the cast specimen dendrite arm spacing and ultimately, its response to solution heat treatment and primary gamma prime aging treatment. It must, therefore, be recognized that much of the creep-rupture results reported herein may have been generated under non-optimized conditions and may be capable of improvement. Improved casting process control may provide casting microstructures more amenable to solution treatment and study to determine the appropriate primary gamma prime aging treatment to provide the optimum gamma prime particle size, which may result in further mechanical property enhancement.

The CMSX-12C composition was designed to provide a calculated N_{v3B} number of 1.70. The alloy Cr content was designed at 2.8% and Co set at 3.5% aim for this alloy. An attractive Ta/W ratio was maintained while Re content was moderate at 5.8%. The alloy's Ai+Ti content was reduced, in comparison to the CMSX-12A and CMSX-12B specimens, to provide improved alloy response to solution procedure.

Similar to the CMSX-10Ga specimen, the CMSX-12C specimen exhibited an improved balance of creep strength for test condition ranging 1800°–2100° F., as reported in Table 21 below.

TABLE 21

CMSX-12C CREEP-RUPTURE							
	RUPTURE TIME	%	%	FINAL CREEP READING		TIME IN HOURS TO REACH	
TEST CONDITION	HOURS	ELONG.	RA	t, hours	% deformation	1.0%	2.0%
1800° F./36.0 ksi	465.2	31.8	21.0	464.5	30.543	173.0	262.4
	518.0	26.1	31.2	517.9	24.947	288.1	334.3
	480.9	28.3	33.6	480.0	27.715	239.7	297.5
	713.3	30.0	28.0	713.2	28.899	455.0	503.7
1850/36.0	237.7	28.2	26.8	237.7	27.054	114.4	145.3
	221.2	22.9	27.3	220.7	22.491	111.3	135.2
	231.7	23.3	24.7	231.0	22.614	121.0	144.7
	338.9	26.2	27.0	337.5	23.256	216.0	236.3
	300.1+			—	—	—	—
	295.2+	33.3	33.5	—	—	—	—
1976/28.1	73.2	20.8	29.1	72.2	17.768	29.3	38.9
	79.0	28.1	31.8	77.4	21.533	31.4	41.4
	83.8	21.6	26.5	82.3	17.860	34.2	43.8
	67.6	31.2	29.8	67.5	24.177	25.5	34.6
	113.0+						
	79.4					30.8	
	76.2					32.8	
	68.8					29.3	
	118.1	26.0	28.0	116.2	23.822	49.3	62.0
	(INTERRUPTED TESTS)			—	—	29.0	—
				—	—	29.4	—
				—	—	32.9	—
1976/18.85 ksi						65.4	
						218.0	
	(INTERRUPTED TESTS)			—	—	271.9	—
				—	—	168.9	—
				—	—	116.4	—
						240.5	
2012/14.5	1001.8	23.6	20.0	1000.7	23.348	249.6	542.8
	865.5	20.7	26.1	864.8	18.807	418.2	569.3
						61.9	
						267.1	
2050/15.0	509.4	13.7	22.3	508.0	12.860	158.1	315.1
	546.4	15.6	23.6	546.4	14.044	323.0	404.0
						180.8	
						44.2	

TABLE 21-continued

	CMSX-12C CREEP-RUPTURE						
	RUPTURE TIME	%	%	FINAL CREEP READING		TIME IN HOURS TO REACH	
TEST CONDITION	HOURS	ELONG.	RA	t, hours	% deformation	1.0%	2.0%
						240.7	
						190.9	
2100/12.0	404.3	11.2	21.6	404.3	8.438	290.1	326.4
	321.7	9.5	15.0	320.4	7.671	156.6	254.1
	545.1	8.2	22.1	542.2	5.351	236.0	452.9
	457.4	8.6	23.4	455.8	6.612	309.3	380.9
2100° F./12.0	371.4+	14.2	17.1	—	—	—	—
1750° F./50.0	446.9+	16.8	20.4	—	—	—	—
1976° F./18.85	476.6+	19.2	27.1	—	—	—	—
	459.9+	30.6	30.2	—	—	—	—
1976° F./28.1 ksi	120.5+	24.1	22.9	—	—	—	—
	99.6+	25.8	29.4	—	—	—	—
2050° F./15.0 ksi	469.8	—	30.8	—	—	—	—
	485.4	—	22.7	—	—	—	—
2012° F./14.5 ksi						638.1	
						521.8	
						267.1	
						61.9	
						395.7	

+Machined From Blade Specimens

With improved casting process controls, this specimen has shown the following 1.0% longitudinal creep strengths, as reported in Table 22 below.

TABLE 22

Test Condition	Time to 1.0% Strain Hrs
1800° F./36.0 ksi	455
2100° F./12.0 ksi	309.3

Both alloys provide similarly greater rupture strength than CMSX-4 alloy at condition to 1976° F. Respective improvements to metal temperature capability are reported below in Table 23.

TABLE 23

Temperature	Approx. Strength Advantage Relative to CMSX-4
1800° F.	40° F.
1850° F.	45° F.
1976° F.	43° F.
Based on 1.0% creep strength, the respective approximate advantages are:	
1800° F.	+46° F.
1850° F.	+60° F.
1976° F.	+55° F.
Note that the comparison is not density corrected.	

For test temperature above 1976° F., the test results indicate that the CMSX-10Ga and CMSX-12C specimens provided slightly lower strength than CMSX-4 alloy. The reduction in strength advantage for these alloys is believed to be the result of TCP phase formation. To address this issue, the alloys CMSX-10Gb, CMSX-10L, CMSX-12Ca, and CMSX-12E, are designed with N_{v3B} number as low as 1.50 (see Table 1) to provide greater phasial stability, and effect much improved high temperature creep-strength while maintaining most of the creep advantage demonstrated for the 1800°–1976° F. test regime.

The CMSX-10Ri and CMSX-12Ri compositions were designed at the 1.91 and 1.92 N_{v3B} levels, respectively. These specimens were subjected to the most extensive testing of properties. They were designed with 2.65% and 3.4% respective Cr levels, with other features remaining similar to the aforementioned alloy design considerations. The properties generated for these two materials confirm the overall invention design concept with the other material iterations able to provide similar physical properties and relatively better blends of mechanical properties.

The CMSX-10Ri and CMSX-12Ri specimens' respective creep-rupture capabilities are reported below in Tables 24 and 25.

TABLE 24

	CMSX-10(Ri) CREEP-RUPTURE						
	RUPTURE TIME	%	%	FINAL CREEP READING		TIME IN HOURS TO REACH	
TEST CONDITION	HOURS	ELONG.	RA	t, hours	% deformation	1.0%	2.0%
1675° F./75.0 ksi	227.3	21.2	33.8	225.4	14.359	52.8	131.5
	231.6	19.3	31.0	231.3	16.671	51.0	125.1
	223.4	17.0	22.3	223.3	15.360	68.5	126.6
1750/50.0	425.9	18.3	33.7	425.6	16.047	303.4	334.7
	428.0	18.4	29.7	427.3	16.229	309.2	343.0
	460.8	17.1	25.7	459.0	15.308	314.7	360.3
1800/36.0	698.5	39.9	34.3	696.8	36.980	492.8	521.5
	676.3	28.3	33.3	674.5	27.221	479.0	513.8
	692.9	38.5	31.3	692.2	36.494	469.3	504.9
1850/36.0	291.2	34.1	33.1	291.1	31.774	194.1	210.4
	260.0	29.3	32.1	258.8	25.321	170.2	186.4
	272.3	34.5	31.8	271.1	30.940	169.3	187.1
1850/27.56	614.0	52.0	42.0	613.5	50.482	365.8	415.5
	576.3	49.7	39.0	575.9	49.183	345.1	368.2
	481.1	40.4	35.4	480.7	38.294	309.3	335.4

TABLE 24-continued

CMSX-10(Ri) CREEP-RUPTURE

TEST CONDITION	RUPTURE TIME HOURS	% ELONG.	% RA	FINAL CREEP READING t, hours	FINAL CREEP READING % deformation	TIME IN HOURS TO REACH 1.0%	TIME IN HOURS TO REACH 2.0%
1976/28.1	76.2	23.5	31.7	75.9	22.130	38.6	46.7
	80.5	19.0	26.3	79.8	14.665	44.3	51.3
	99.7	26.2	28.1	98.9	23.480	40.4	54.0
	(INTERRUPTED TESTS)					41.4	—
						37.0	—
						40.5	—
1976/18.85	265.6	29.5	35.7	264.7	29.010	158.7	184.8
	278.8	51.4	38.8	278.1	46.026	82.0	155.0
	(INTERRUPTED TESTS)					139.7	—
						128.8	—
						100.1	—
2012/14.5	490.8	40.2	33.5	490.5	37.678	286.5	335.3
	447.0	37.0	41.5	445.0	32.814	291.4	319.9
	(INTERRUPTED TESTS)			—	—	113.5	—
				—	—	205.7	—
				—	—	202.2	—
2050/15.0	251.9	33.6	35.9	250.0	25.559	100.0	149.5
	318.9	27.1	30.0	318.2	23.149	177.5	221.2
	(INTERRUPTED TESTS)			—	—	181.0	—
				—	—	95.5	—
				—	—	34.5	—
2100/12.0	400.3	17.9	27.2	400.1	17.877	102.8	225.0
	362.1	15.3	22.9	361.8	14.986	125.7	217.2
	389.5	19.9	24.0	388.2	19.510	41.1	180.7

TABLE 25

CMSX-12(Ri) CREEP-RUPTURE

TEST CONDITION	RUPTURE TIME HOURS	% ELONG.	% RA	FINAL CREEP READING t, hours	FINAL CREEP READING % deformation	TIME IN HOURS TO REACH 1.0%	TIME IN HOURS TO REACH 2.0%
1675° F./75.0 ksi	209.8	22.3	23.1	209.3	19.958	2.6	46.3
	191.4	14.3	17.4	189.7	12.483	1.6	42.5
	189.6	22.0	22.8	188.3	19.080	1.5	22.3
1750/50.0	448.1	26.7	26.6	447.9	26.054	302.3	335.5
	403.1	19.0	26.9	401.9	18.566	210.0	290.2
	435.0	19.4	26.9	434.4	18.503	89.1	284.1
1800/36.0	604.5	34.7	29.9	604.3	34.170	349.4	407.1
	583.6	37.0	32.0	581.3	30.443	391.3	420.6
	627.0	25.3	29.7	627.0	24.417	412.4	455.8
1850/36.0	302.9	33.1	31.3	301.7	29.034	198.9	215.1
	314.4	32.0	27.1	312.7	27.479	201.4	220.2
1976/28.1	90.0	19.7	29.2	88.5	16.627	33.9	48.8
	91.5	30.3	31.9	90.6	29.001	37.3	47.9
	68.6	35.3	32.2	68.4	28.869	17.3	27.6
	(INTERRUPTED TESTS)					43.7	—
						41.4	—
						38.7	—
2012/14.5	324.1	31.4	30.8	323.9	24.403	160.1	207.7
	481.4	30.9	31.9	481.1	29.581	129.9	299.6
	551.7	29.9	31.1	549.2	25.622	304.4	375.5
	(INTERRUPTED TESTS)					256.1	—
						182.8	—
						101.5	—
2050/15.0	243.4	36.1	35.0	243.3	20.614	143.1	174.2
2100/12.0	374.8	12.1	20.3	374.7	11.743	166.6	280.4
	463.6	15.4	25.9	463.3	13.594	245.7	363.3
	488.0	20.3	25.9	487.1	19.550	25.7	118.9

The method and results of W and Re microstructural segregation investigation undertaken on fully solutioned and partially solutioned CMSX-12Ri test specimens are reported in Table 26 below. The investigation indicated that it is desirable to minimize the amount of microstructure-contained residual eutectic and that for fully solutioned specimens, the solution treatments developed for the invention are successful in minimizing elemental segregation, which is important in attaining optimized mechanical properties and microstructural stability.

TABLE 26

Alloy: CMSX-12 Ri
Test Specimen: ⅜" Diameter Solid Bar
Specimen Condition: Fully Solutioned
Solutioned with 2.0% Residual Eutectic
Analyses Method: Microprobe Analyses
+Random array of 350 points across a section at right angles to the growth direction
+Seven line scans, 51° apart, 50 point analyses per line
The standard deviation of the W and Re measurements are the measure of homogeneity

Results:

TABLE 26-continued

CMSX-12 Ri	Standard Deviations W	Re
Fully Solutioned	0.27	0.50
2% Residual Eutectic	0.36	0.90
Comparison	0.57	0.60
Typical CMSX-4		

Table 27 below reports results of burner rig hot corrosion test undertaken with the CMSX-12Ri specimen. The measurements were taken at the bar location which experienced the maximum attack, i.e., 1652° F. location, with the results showing the DS MAR M 002 alloy experienced approximately 20× more metal loss than the CMSX-12Ri specimen. Visual observation showed a similar result for the CMSX-10Ri alloy. Both CMSX-10Ri alloy and CMSX-12Ri alloy showed similar resistance to attack as CMSX-4 alloy based on visual specimen review at 60, 90 and 120 hours.

TABLE 27

HOT CORROSION

METHOD
- +Burner Rig
  1742° F. (950° C.)
  2 ppm salt, standard fuel
- +Measurements taken at point of maximum attack which was at 1652° F. (900° C.)
- +Measurements reported were taken at the average minimum diameter of useful metal

RESULTS
- +90 Hour Test

Alloy	Initial Dia.	Post Test Useful Dia.	Metal Loss Per Side
DS Mar M 002	6.88 mm	5.14 mm	.87 mm (.034")
CMSX-12Ri	6.86 mm	6.78 mm	.04 mm (.0016")

Table 28 below reports the results of cyclic oxidation tests undertaken at 2012° F. with March 1 gas velocity. The CMSX-12Ri specimen was similarly resistant to oxidation attack at 2012° F., however, it was not as good as CMSX-4 at approximately 1886° F. exposure.

TABLE 28

Cyclic Oxidation Test

- •15 Minute Cycles to 2012° F. (1100° C.), Cooled to Ambient Between Cycles
  Mach 1 Gas Velocity
- •89 Hours Total With 77 Hours at 2012° F.

RESULT:	at 1100° C.	CMSX-12 Ri Approx. 0.1 mm loss per side for every 300 cycles CMSX-4 Approx. 0.1 mm loss per side for every 380 cycles
	at 1030° C.	CMSX-12 Ri Approx. .105 mm loss per side after 355 cycles CMSX-4 Approx. .03 mm loss per side after 355 cycles

CMSX-12Ri elevated temperature tensile data is reported in Table 29 below, while the results of impact tests are reported in Table 30 below. The CMSX-12Ri elevated temperature impact strength minimum is similar to CMSX-4 and its maximum occurring at 1742° F., is better.

TABLE 29

TENSILE DATA
CMSX-12 Ri Alloy

Test Temp °F.	LAUE	0.1% Yld ksi	0.2% Yld ksi	UTS ksi	Elong %	RA %
1382	2.3°	150.0	160.8	188.7	13	14
1382	2.3°	153.6	165.1	190.0	13	15
1562	6.2°	136.5	130.8	152.3	27	24
1562	6.2°	135.0	128.9	160.1	25	23
1742	5.6°	92.7	89.2	125.3	24	30
1742	5.6°	99.9	106.2	129.2	24	32
1922	3.8°	69.5	74.3	104.1	19	36
1922	3.8°	72.4	77.6	106.0	19	36

TABLE 30

IMPACT DATA
CMSX-12 Ri
0.35 Inch Diameter Plain Cylindrical Specimens

	Test Temperature, °F. 1382	1562	1742	1922
CMSX-12 Ri (1 only)	26 J	20 J	60 J	32 J
CMSX-4 (Ave. of 4)	26 J	21 J	42 J	45 J

Further Impact Property Comparison
- •CMSX-2-Min. Impact Strength 16.5 Joules
- •SRR 99-Min. Impact Strength 20 Joules

The results of CMSX-12Ri low cycle fatigue tests undertaken at 1382° F. and 1742° F. test conditions, with R=0, are reported in Table 31 below. The data indicates that CMSX-12Ri performance is similar to CMSX-4 at 1382° F. condition, while the alloy exhibits approximately 2.5 times the typical CMSX-4 life at 1742° F. condition.

TABLE 31

LOW CYCLE FATIGUE
CMSX-12 Ri Alloy
R = 0 (zero to maximum stressing)

1382° F. (750° C.) PEAK STRESS ksi (MPa)	Cycles	1742° F. (950° F.) PEAK STRESS ksi (MPa)	Cycles
142 (980)	8686	110 (760)	4427
130 (900)	11950	99 (680)	15510
125 (860)	20810	87 (600)	37430
119 (820)	>100000	75 (520)	92580

- •Performance is similar to CMSX-4 at 1382° F. (750° C.)
- •Compared to CMSX-4, at 1742° F. (950° C.) and in the 20000 cycle region, CMSX-12Ri exhibits 2.5 times life or 15% on strength.

Notched low cycle fatigue test results show the CMSX-12Ri is 2½ times better than CMSX-4 out to about 3000 cycles, while at 50000 cycles and above, the alloy performance is similar to CMSX-4. The results of these tests performed at 1382° F., K_t=2.0 and R=0 test condition, are reported in Table 32 below.

TABLE 32

NOTCHED LOW CYCLE FATIGUE
CMSX-12Ri Alloy
1382° F. (750° C.), K_t = 2.0, R = 0

PEAK STRESS ksi (MPa)	CYCLES
113.13 (780)	4879
107.33 (740)	9784
95.72 (660)	28470
84.12 (580)	49810
81.22 (560)	
78.32 (540)	>115,000

TABLE 32-continued

NOTCHED LOW CYCLE FATIGUE
CMSX-12Ri Alloy
1382° F. (750° C.), K_t = 2.0, R = 0

PEAK STRESS ksi (MPa)	CYCLES
75.42 (520)	>115,000

•Results are 2½ times better than CMSX-4 out to about 30000 cycles.
•Results are similar to CMSX-4 at 50000 cycles, and above.

High cycle fatigue test results for the CMSX-10Ri alloy are reported in Table 33 below. For 1742° F., 100 Hz, R=0 test condition, the alloy exhibited about 2½ times the typical CMSX-4 lives.

TABLE 33

HIGH CYCLE FATIGUE CMSX-10Ri Alloy
1742° F. (950° C.), 100 Hz., R = 0

PEAK STRESS ksi (MPa)	CYCLES (N_f)
81.22 (560)	15.2×10^6
92.82 (640)	3.59×10^6
104.43 (720)	0.6×10^6

*Lives are 2½ times better than CMSX-4

The CMSX-10Ri and CMSX-12Ri test data indicates that adequate hot corrosion and oxidation resistance can be achieved with extremely low alloy chromium content. Additionally, extremely good thermo-mechanical fatigue tensile and impact strengths are apparent with the superalloys of this invention.

The results of alloy specimen density measurements are reported in Table 34 below.

TABLE 34

SINGLE CRYSTAL ALLOY DENSITY DATA

ALLOY	DENSITY Lbs/In^3
CMSX-10A	.324
CMSX-10B	.324
CMSX-10C	.325
CMSX-10D	.325
CMSX-10E	.325
CMSX-10F	.323
CMSX-10G	.322
CMSX-10Ga	.322
CMSX-10H	.324
CMSX-10I	.322
CMSX-10Ia	.322
CMSX-10J	.327
CMSX-10Gb (10K)	.329
CMSX-12A	.323
CMSX-12B	.325
CMSX-12C	.326
CMSX-12Ca (12D)	.326
CMSX-10Ri	.326
CMSX-10 Ri	.323

The alloys of this invention are amenable to HIP processing. Specimens HIP treated as reported in Table 35 below, showed nearly complete pore closure and absence from incipient melting.

TABLE 35

HIP condition
1. Heat Specimens in the HIP vessel to 2455° F. at mininum Argon pressure (approximately 1500 psi) and hold for 4 hours while maintaining 2455° F./1500 psi condition.
2. While maintaining the 2455° F. operating temperature, increase the Argon pressure over 1 hour to 20 ksi. Soak specimens at 2455° F./20

TABLE 35-continued

HIP condition
ksi condition fo 4 hours.

While this invention has been described with respect to particular embodiments thereof, it is apparent that numerous other forms and modifications of this invention will be obvious to those skilled in the art. The appended claims and this invention generally should be construed to cover all such obvious forms and modifications which are within the true spirit and scope of the present invention.

What is claimed is:

1. A nickel-based superalloy comprising the following elements in percent by weight:

Rhenium	about 5.0–7.0
Chromium	about 1.8–4.0
Cobalt	about 1.5–9.0
Tantalum	about 7.0–10.0
Tungsten	about 3.5–7.5
Aluminum	about 5.0–7.0
Titanium	about 0.1–1.2
Columbium	about 0–0.5
Molybdenum	about 0.25–2.0
Hafnium	about 0–0.15
Carbon (Incidental Impurity)	about 0–0.04
Nickel + Other Incidental Impurities	balance

said superalloy having a phasial stability number N_{v3B} less than about 2.10.

2. The superalloy of claim **1** further comprising the following elements in percent by weight:

Boron	about 0–0.01
Yttrium	about 0–0.01
Cerium	about 0–0.01
Lanthanum	about 0–0.01

3. The superalloy of claim **1** further comprising the following elements in percent by weight:

Manganese	about 0–0.04
Silicon	about 0-0.05
Zirconium	about 0-0.01
Sulfur	about 0-0.001
Vanadium	about 0-0.10

4. The superalloy of claim **1** wherein said superalloy has a phasial stability number N_{v3B} less than 1.85.

5. The superalloy of claim **1** wherein said superalloy has a chromium content of from about 1.8 to about 3.0 percent by weight.

6. The superalloy of claim **1** wherein said superalloy has a rhenium content of from about 5.5 to about 6.5 percent by weight.

7. The superalloy of claim **1** wherein said superalloy has a cobalt content of from about 2.0 to about 5.0 percent by weight.

8. The superalloy of claim **1** wherein said superalloy has an increased resistance to creep under high stress, high temperature conditions up to about 1975° F.

9. A single crystal article made from the superalloy of claim **1**.

10. The single crystal article of claim **9** wherein the article is a component for a turbine engine.

11. The article of claim 10 wherein the component is a gas turbine blade or gas turbine vane.

12. A nickel-based superalloy comprising the following elements in percent by weight:

Rhenium	5.5–6.5
Chromium	1.8–3.0
Cobalt	2.0–5.0
Tantalum	8.0–10.0
Tungsten	3.5–6.5
Aluminum	5.3–6.5
Titanium	0.2–0.8
Columbium	0–0.3
Molybdenum	0.25–1.5
Hafnium	0.02–0.05
Carbon (Incidental Impurity)	about 0–0.04
Nickel + other Incidental Impurities	balance

said superalloy having a phasial stability number N_{v3B} less than about 1.75.

13. The superalloy of claim 12 further comprising the following elements in percent by weight:

Boron	0–0.01
Yttrium	0–0.01
Cerium	0–0.01
Lanthanum	0–0.01

14. The superalloy of claim 12 further comprising the following elements in percent by weight:

Manganese	0–0.04
Silicon	0–0.05
Zirconium	0–0.01
Sulfur	0–0.001
Vanadium	0–0.10

15. A single crystal article made from the superalloy of claim 12.

16. A single crystal casting to be used under high stress, high temperature conditions characterized by an increased resistance to creep under such conditions, said casting being made from a nickel-based superalloy comprising the following elements in percent by weight:

Rhenium	about 5.0–7.0
Chromium	about 1.8–4.0
Cobalt	about 1.5–9.0
Tantalum	about 7.0–10.0
Tungsten	about 3.5–7.5
Aluminum	about 5.0–7.0
Titanium	about 0.1–1.2
Columbium	about 0–0.5
Molybdenum	about 0.25–2.0
Hafnium	about 0–0.15
Carbon (Incidental Impurity)	about 0–0.04
Nickel + other Incidental Impurities	balance

Rhenium	about 5.0–7.0
Chromium	about 1.8–4.0
Cobalt	about 1.5–9.0
Tantalum	about 7.0–10.0
Tungsten	about 3.5–7.5
Aluminum	about 5.0–7.0
Titanium	about 0.1–1.2
Columbium	about 0–0.5
Molybdenum	about 0.25–2.0
Hafnium	about 0–0.15

-continued

Carbon (Incidental Impurity)	about 0–0.04
Nickel + Other Incidental Impurities	balance

said superalloy having a phasial stability number N_{v3B} less than about 2.10.

17. The single crystal casting of claim 16 wherein said superalloy further comprises the following elements in percent by weight:

Boron	about 0–0.01
Yttrium	about 0–0.01
Cerium	about 0–0.01
Lanthanum	about 0–0.01

18. The single crystal casting of claim 16 further comprising the following elements in percent by weight:

Manganese	about 0–0.04
Silicon	about 0–0.05
Zirconium	about 0-0.01
Sulfur	about 0–0.001
Vanadium	about 0–0.10

19. The single crystal casting of claim 16 wherein said superalloy has a phasial stability number N_{v3B} less than 1.85.

20. The single crystal casting of claim 16 wherein said superalloy has a chromium content of from about 1.8 to about 3.0 percent by weight.

21. The single crystal casting of claim 20 wherein said superalloy has a rhenium content of from about 5.5 to about 6.5 percent by weight.

22. The single crystal casting of claim 21 wherein said superalloy has a cobalt content of from about 2.0 to about 5.0 percent by weight.

23. The single crystal casting of claim 16 wherein said superalloy has an increased resistance to creep under high stress, high temperature conditions up to about 1975° F.

24. The single crystal casting of claim 16 wherein said casting has been aged at a temperature of from about 1950° F. to about 2125° F. for about 1 to about 20 hours.

25. The single crystal casting of claim 16 wherein said casting is a component for a turbine engine.

26. The single crystal casting of claim 16 wherein said casting is a gas turbine blade.

27. The single crystal casting of claim 16 wherein said casting is a gas turbine vane.

28. A single crystal casting to be used under high stress, high temperature conditions up to about 1975° F. characterized by an increased resistance to creep under such conditions, said casting being made from a nickel-based superalloy comprising the following elements in percent by weight:

Rhenium	about 5.5–6.5
Chromium	about 1.8–3.0
Cobalt	about 2.0–5.0
Tantalum	about 8.0–10.0
Tungsten	about 3.5–6.5
Aluminum	about 5.3–6.5
Titanium	about 0.2–0.8
Columbium	about 0–0.3
Molybdenum	about 0.25–1.5

-continued

Hafnium	about 0.02–0.05
Carbon	about 0–0.04
Boron	about 0–0.01
Yttrium	about 0–0.01
Cerium	about 0–0.01
Lanthanum	about 0–0.01
Manganese	about 0–0.04
Silicon	about 0–0.05
Zirconium	about 0–0.01
Sulfur	about 0–0.001
Vanadium	about 0–0.10

-continued

Nickel	balance

said superalloy having a phasial stability number N_{v3B} less than about 1.75.

29. The single crystal casting of claim **28** wherein said casting has been aged at a temperature of from 1950° F. to 2125° F. for 1 to 20 hours.

30. The single crystal casting of claim **28** wherein said casting is a component for a turbine engine.

31. The single crystal casting of claim **28** wherein said casting is a gas turbine blade.

32. The single crystal casting of claim **28** wherein said casting is a gas turbine vane.

* * * * *